運輸省港湾技術研究所 (25th Anniversary Issue)

港湾技術研究所報告

REPORT OF THE PORT AND HARBOUR RESEARCH INSTITUTE

MINISTRY OF TRANSPORT

VOL. 26 NO. 5 DEC. 1987

NAGASE, YOKOSUKA, JAPAN

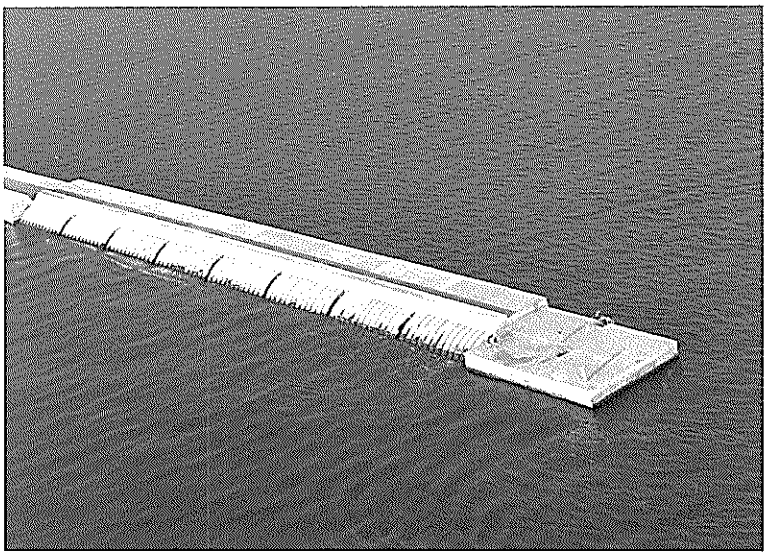

Curved Slit Caisson Breakwater

View of curved slit caisson breakwater completed in the construction at the port of Funakawa. (Courtesy of Akita Port Construction Office, the First District Port Construction Bureau, Ministry of Transport)

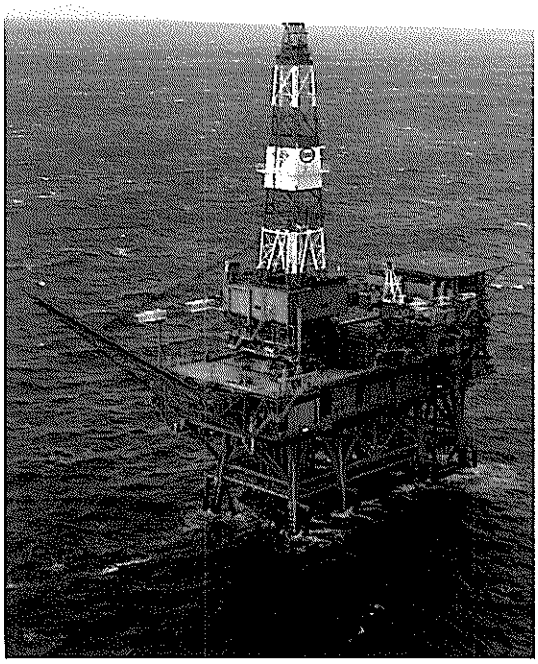

Facilities for Ocean Directional Wave Measurement

Four step type wave gauges and a two-axis directional current meter with a pressure sensor are installed on the legs of an offshore oil rig. They are operated simultaneously for detailed directional wave analysis.

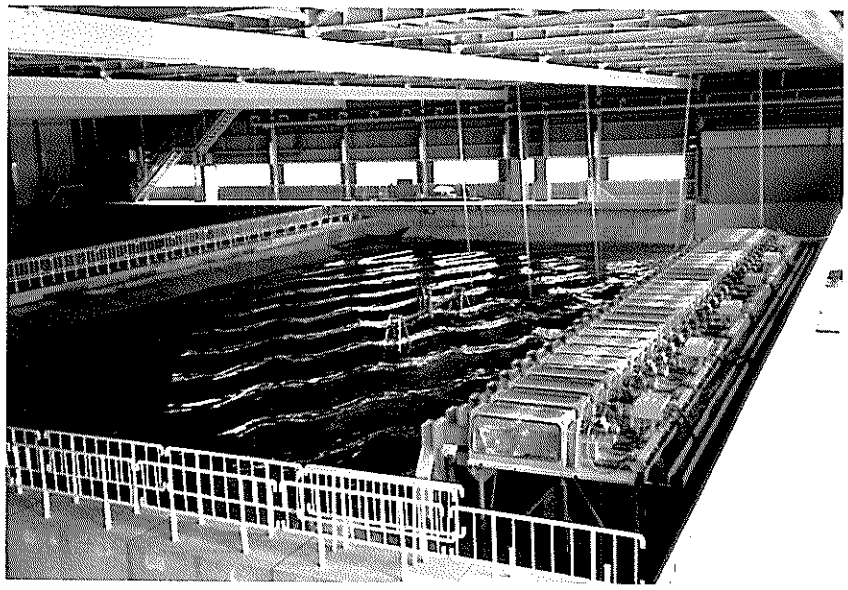

Serpent-type Wave Generator

The photograph shows the serpent-type wave generator in the short-crested wave basin and the superimposition state of two different oblique waves generated by the generator.

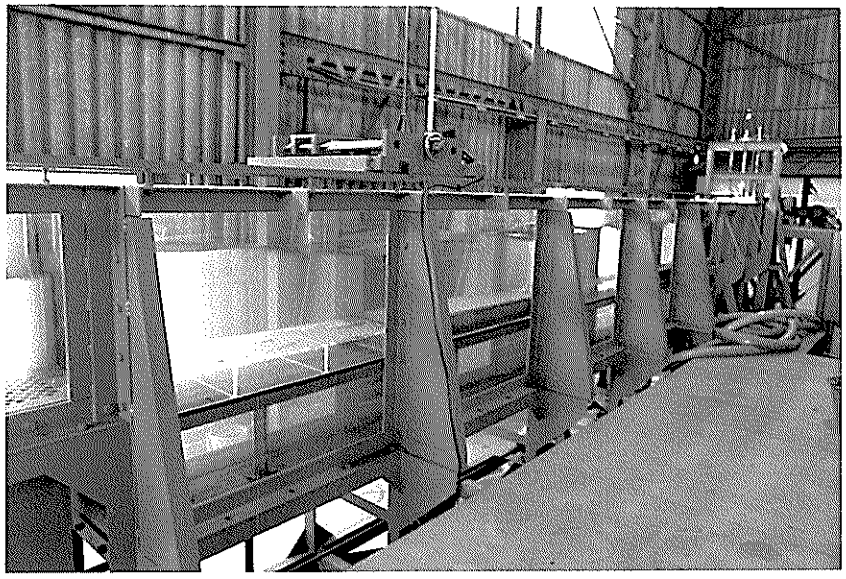

Wave-soil Tank

The experiments concerning the wave-soil interactions are conducted in this tank. The soil tank and the test section are located at the center of the tank. A movable floor is provided at the bottom of the test section and the level of the interface of mud layer and water can easily be adjusted to the level of the flume bottom.

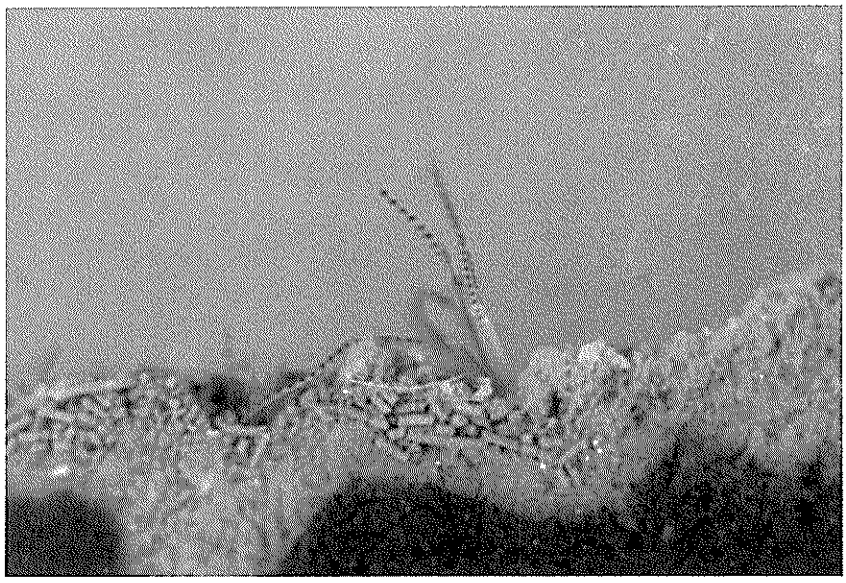

Pararionospio Pinnata

The biomass of benthos is one of the most sensitive indices to know the effect of sea-bed sediment treatments on the marine environmental improvement. The picure shows a kind of benthos, *pararionospio pinnata,* which preferentially exists in the polluted sea-bed.

Breakwater Damaged by Storm

This photograph shows a breakwater damage by a storm.
The breakwater is of the composite type with concrete caisson on a rubble mound. Two caissons were severly damaged due to the instability of a rubble mound.

Nondestructive Evaluation of Pavement

Nondestructive methods for evaluating the load carrying capacity of airport concrete pavements have been developed by using Falling Weight Deflectometer(FWD).

Seismic Damage to Gravity Quaywall

The 1983 Nipponkai-Chubu earthquake(Magnitude : 7.7)caused serious damage to port facilities in northern part of Japan. This photo shows the damage to gravity quaywall. The concrete cellular block walls were collapsed and completely submerged.

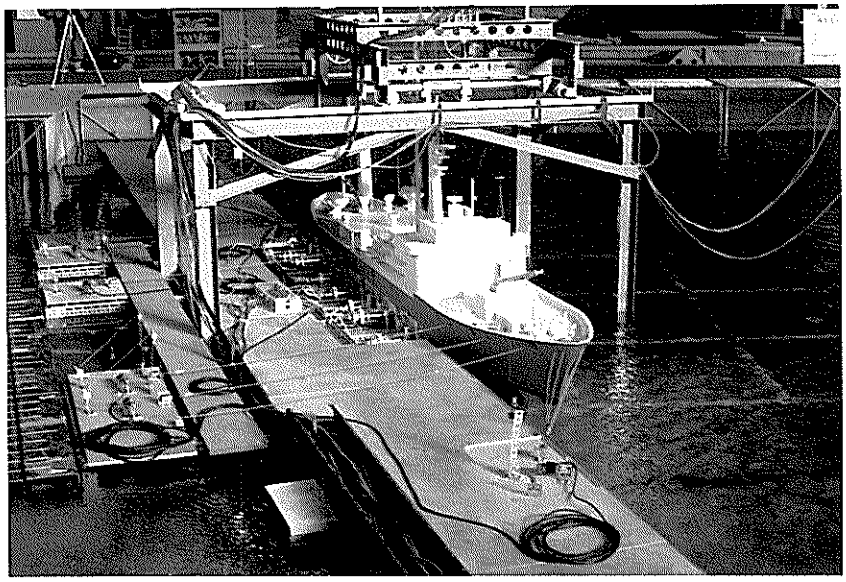

Model Experiment of Mooring Ship

Model ship is moored at a quay wall with fenders and mooring ropes subjected to gusty wind and/or irregular waves.

Vessel Congestion in Japan

As Japan is surrounded by the sea, there are many crowded water areas with various sizes and types of vessels. Arround there, many construction works were planned such as ports and harbours, off-shore airports, huge bridges and so on, so that many marine traffic observations and marine traffic simulations have been carried out.

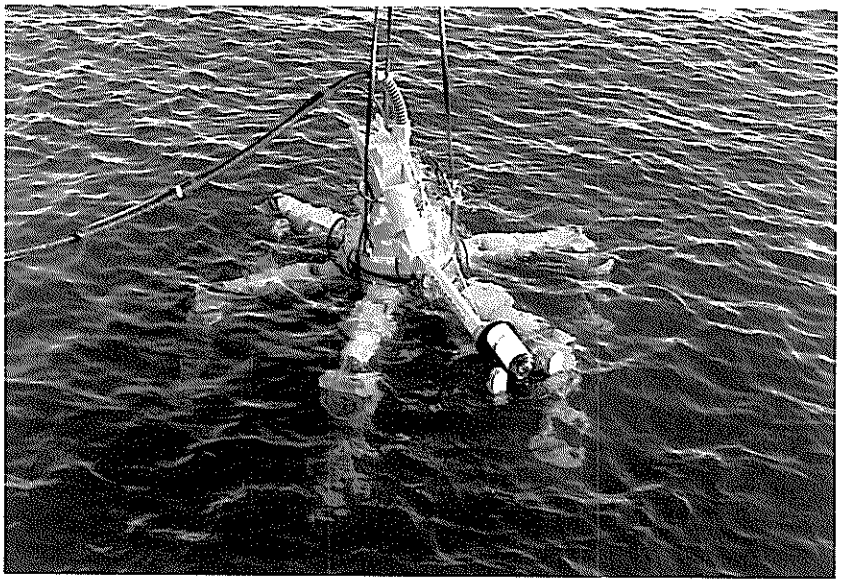

Underwater Inspection Robot

This is the six-legged articulated underwater inspection robot named "AQUAROBOT". The robot controlled by a computer can walk on uneven sea bed without making water muddy.

Foreword

The Port and Harbour Research Institute is a national laboratory under the Ministry of Transport, Japan. It is responsible for solving various engineering problems related to port and harbour projects so that governmental agencies in charge of port development can execute the projects smoothly and rationally. Its research activities also cover the studies on civil engineering facilities of air ports.

Last April we have celebrated the 25th anniversary of our institute because the present organization was established in 1962, though systematic research works on ports and harbours under the Ministry of Transport began in 1946. As an event for the celebration, we decided to publish a special edition of the Report of the Port and Harbour Research Institute, which contains full English papers only. These papers are so selected to introduce the versatility of our activities and engineering practices in Japan to overseas engineers and scientists. It is also intended to remedy to a certain extent the information gap between overseas colleagues and us.

The reader will find that our research fields cover physical oceanography, coastal and ocean engineering, geotechnical engineering, earthquake engineering, materials engineering, dredging technology and mechanical engineering, planning and systems analysis, and structural analysis. Such an expansion of the scope of research fields has been inevitable, because we are trying to cover every aspect of technical problems of ports and harbours as an integrated body.

The present volume contains eleven papers representing six research divisions of the institute. The materials introduced in these papers are not necessarily original in strict sense, as some parts have been published in Japanese in the Reports or the Technical Notes of the Port and Harbour Research Institute. Nevertheless they are all original papers in English and are given the full format accordingly. We expect that they will be referred to as usual where they deserve so.

It is my sincere wish that this special edition of the Report of the Port and Harbour Research Institute will bring overseas engineers and scientists more acquainted with our research activities and enhance the mutual cooperation for technology development related to ports and harbours.

December 1987
Yoshimi Goda
Director General

港湾技術研究所報告 (REPORT OF P. H. R. I.)
第26巻 第5号 (Vol. 26, No. 5) 1987年12月 (Dce. 1987)

目　　次 (CONTENTS)

REPORT OF THE PORT AND
HARBOUR RESEARCH INSTITUTE
Vol. 26, No. 5 (Dec. 1987)

2. Estimation of Directional Spectrum using the Bayesian Approach, and its Application to Field Data Analysis#

Noriaki HASHIMOTO*
Koji KOBUNE**
Yutaka KAMEYAMA***

Synopsis

Directional spectra are the fundamental properties of sea waves, which express the energy distribution as a function of wave frequency and the direction of wave propagation. So far, several methods for estimating directional spectra for various types of ocean wave measurements have been proposed but no method has yet taken into consideration the errors emerging from estimating cross-power spectra that forms the base information for the directional spectral estimation. These errors often lead to ill-conditioned directional spectra depending on the arrangement and the number of wave probes.

Therefore, it is of great importance to develop a method which gives an accurate estimate of the directional spectrum even though the cross-power spectra are contaminated with estimation errors.

Initially, the report discusses several methods for estimating directional spectra from the viewpoint of considering the estimate instability caused by cross-power spectral estimation errors. Secondly, a new directional spectral estimation method using the Bayesian approach is proposed. The Bayesian approach was originally introduced by *Akaike* in the field of regression analysis problems where the number of the parameters to be determined was large, when compared with the sample size.

The proposed method is examined for numerical simulation data, and the validity of the method is discussed. Some examples of the directional spectra estimated from field observation data attained at an offshore oil rig utilizing 7 wave probes are also shown in this report.

The major conclusions of the report are:

1) The proposed method can be applied to arbitrarily mixed instrument array measurements.
2) The Bayesian model has a higher resolution power than other existing methods for estimating the directional spectrum.
3) The Bayesian model is better method for estimating directional spectra from the cross-power spectra contaminated with estimation errors.
4) The Bayesian model is more adaptable to reformulation of estimation equations as the study of structures of directional wave spectrum progresses.

This report is a translated and re-edited version of the report in Vol. 26, No. 2 of the Rept. of P.H.R.I., under the title "Estimation of directional spectrum from a Bayesian Approach" by N. Hashimoto.

* Senior Research Engineer, Hydraulic Engineering Division.
** Chief, Coastal Observation Laboratory, Hydraulic Engineering Division.
*** Member, Coastal Observation Laboratory Hydraulic Engineering Division.

港湾技術研究所報告
第26巻 第5号 (1987.12)

2. ベイズ型モデルを用いた方向スペクトル推定法および現地観測データへの適用#

橋本典明*・小舟浩治**・亀山豊***

要旨

海の波の基本的性質を表示するために，波のエネルギーが周波数および方向角に対して分布している状態を表示する方向スペクトルが用いられる。方向スペクトルを推定する方法としては，これまでにも，いくつかの方法が提案されている。しかしながら，いずれの方法も，方向スペクトルを推定するために必要なクロススペクトルに，推定誤差が含まれる場合については，考慮されていない。

このため，観測波動量の種類や数，配置によっては，クロススペクトルの推定誤差に起因して，異常な方向スペクトルが推定される場合があり，必ずしも分解能の良い，安定した方向スペクトルが得られるとは限らない。

したがって，これまでのように少ない観測波動量から精度の良い方向スペクトルを推定することのみならず，観測誤差，推定誤差の影響を受けにくく，安定した方向スペクトルを推定できる方法を開発する必要がある。

そこで，著者らは既往の方向スペクトルの推定理論を，クロススペクトルの推定誤差に対する不安定性の立場から再考し，上記の問題点を解消する新しい方向スペクトルの推定理論として，ベイズ型モデルを導入した方向スペクトルの推定理論を検討した。ベイズ型モデルを用いた方向スペクトルの推定法は，波浪の物理特性を考慮した物理的な推定法であり，極めて柔軟性に富む方法である。

本報告では，ベイズ型モデルを用いた方向スペクトル推定法について，その理論的背景，理論式の定式化，および，数値シミュレーションにより，その適用性を検討した結果について報告している。さらに，この手法を用いて，水深150mの石油掘削プラットフォーム上で観測した，7成分波浪観測データを用いた方向スペクトル解析結果も紹介している。

得られた主な結果は次の通りである。

1) 本方法は任意の波動量に適用可能である。しかしながら，二方向波浪のような複雑な方向スペクトルに対しては4成分以上の波動量が必要である。
2) 本方法による方向スペクトルの推定精度は，既往の方向スペクトル推定法に比べて，極めて良い。
3) 本方法はクロススペクトルの推定誤差の影響を受けにくく，安定した方向スペクトルを推定可能である。
4) 本方法は，その推定式の中に，今後の方向スペクトルの研究成果を直接盛り込むことができる，柔軟性に富む推定法である。

本報告は，港湾技術研究所報告，第26巻第2号に発表した「ベイズ型モデルを用いた方向スペクトルの推定」を英訳し，現地データの解析例を追加したものである。
* 水工部 主任研究官（波浪統計解析担当）
** 水工部 海象観測研究室長
*** 水工部 海象観測研究室

Contents

1. Introduction

Directional spectra are the fundamental properties of ocean waves expressing the energy distribution of random ocean waves as a function of the wave frequency and the direction of wave propagation. Many efforts have been made to estimate directional spectra on the bases of point measurements utilizing various wave probes, and several methods have been proposed to improve the directional resolution of the estimation.

These methods are based on a mathematical relationship between the directional spectrum and the cross-power spectra (*i.e.* the cross-power spectra are equal to the Fourier Transformation of the directional spectrum with respect to the wave number vector). The cross-power spectra are computed from time series records of various wave properties. In practice, wave records are often contaminated with noises. This leads to errors in the cross-power spectral estimation. Thus, the estimate of the directional spectrum is often biased by the noises and the errors associated with the observed cross-power spectra.

However, no current methods take into account the existence of such errors. The directional spectrum is estimated only to satisfy the above mentioned relationship with the observed cross-power spectra, and this may be one of the causes of estimates of the directional spectrum sometimes resulting in poorly conditioned shape, *i.e.* negative values or zigzags, for instance.

The same type of problems are seen in the field of the regression analysis of sample data to determine a regression model which best approximates the observed data. In order to overcome these difficulties, *Akaike*[1] introduced a Bayesian model which better approximates the sample data, and which is compatible with an a priori condition subsistent in the phenomenon to be analyzed.

The estimation of the directional spectrum can be considered as a regression analysis to find the most suitable model from limited data. Therefore, the Bayesian approach should be useful to obtain the most reasonable model (directional spreading function) which best approximates the sample (cross-power spectrum) and which also conforms to the subsistent nature of the physical phenomenon, *i.e.* continuous and smooth variation of its value. This is accomplished by maximizing the likelihood of the model with the a priori condition that the directional spreading function varies smoothly over the wave direction.

In the practical computation, another parameter which is called a hyperparameter, is introduced to consider the balance of the two requirements imposed on the model: to maximize the likelihood of the model and to maintain the smoothness of the model. In order to select the most suitable value of the hyperparameter for the given cross-power spectra, the ABIC[1] (*Akaike's Bayesian Information Criterion*) is also introduced as a criterion to determine the most suitable model.

The report initially discusses how ill-conditioned estimates are obtained when current methods are employed. Secondly, the idea of the Bayesian approach is briefly reviewed, and proposed a new method to overcome the shortcomings of the current methods[2].

The proposed method is examined by numerical simulations, and its application to a practical directional wave analysis is also presented with the data recently recorded on an offshore oil rig at a water depth of 150 meters.

2. Literature Survey for the Estimation of Directional Spectrum

2.1 Fundamental equation related to directional spectrum[3),4)]

The relationship between the cross-power spectrum for a pair of arbitrary wave properties and the wave number-frequency spectrum (which is called the directional spectrum as a function of wave number and frequency hereafter) is introduced by *Isobe et al.*[5)] The relationship shows that the Fourier Transformation of the product of the transfer function of respective wave property and the directional spectrum given as a function of wave number and frequency is equal to the cross-power spectrum, and is expressed as the following equation:

$$\Phi_{mn}(\sigma)=\int_k H_m(\boldsymbol{k},\sigma)H_n^*(\boldsymbol{k},\sigma)\exp\{-i\boldsymbol{k}(\boldsymbol{x}_n-\boldsymbol{x}_m)\}S(\boldsymbol{k},\sigma)d\boldsymbol{k} \tag{1}$$

where σ is the angular frequency, $\boldsymbol{k}$ is the wave number vector, $\Phi_{mn}(\sigma)$ is the cross-power spectrum between the m-th and the n-th wave properties, $H_m(\boldsymbol{k},\sigma)$ is the transfer function from the water surface elevation to the m-th wave property, i is the imaginary unit, $\boldsymbol{x}_m$ is the location vector of the wave probe for the m-th wave property, $S(\boldsymbol{k},\sigma)$ is the directional spectrum as a function of wave number and frequency, and the superscript * denotes the conjugate complex.

Since the wave number k is interrelated with the frequency f by the dispersion equation (2),

$$\sigma^2=(2\pi f)^2=gk\tanh kd \tag{2}$$

the directional spectrum can be expressed as a function of the frequency and the direction of wave propagation. Thus, Eq. (1) can be rewritten as follows:

$$\Phi_{mn}(f)=\int_0^{2\pi} H_m(f,\theta)H_n^*(f,\theta)[\cos\{k(x_{mn}\cos\theta+y_{mn}\sin\theta)\} -i\sin\{k(x_{mn}\cos\theta+y_{mn}\sin\theta)\}]S(f,\theta)d\theta \tag{3}$$

where θ is the direction of the wave propagation, $x_{mn}=x_n-x_m$, $y_{mn}=y_n-y_m$, and $S(f,\theta)$ is the directional spectrum.

The directional spectrum $S(f,\theta)$ is often expressed as a product of the frequency spectrum and the directional spreading function.

$$S(f,\theta)=S(f)G(\theta|f) \tag{4}$$

where, $S(f)$ is the frequency spectrum and $G(\theta|f)$ is the directional spreading function. The directional spreading function takes non-negative values and satisfies the following relationship.

$$\int_0^{2\pi} G(\theta|f)d\theta=1 \tag{5}$$

In the other expression,

$$\int_0^{2\pi} S(f,\theta)d\theta=S(f) \tag{6}$$

The transfer function $H_m(f,\theta)$ in Eq. (3) is generally expressed in the form

$$H_m(f,\theta)=h_m(f)\cos^{\alpha_m}\theta\sin^{\beta_m}\theta \tag{7}$$

Table 1 Transfer function from small amplitude wave theory[5)]

MEASURED QUANTITY	SYMBOL	$h(k,\sigma)$	α	β
Water surface elevation	η	1	0	0
Excess pressure	p	$\rho g\frac{\cosh kz}{\cosh kd}$	0	0
Vertical water surface velocity	η_t	$-i\sigma$	0	0
Vertical water surface acceleration	η_{tt}	$-\sigma^2$	0	0
Surface slope (x)	η_x	ik	1	0
Surface slope (y)	η_y	ik	0	1
Water particle velocity (x)	u	$\sigma\frac{\cosh kz}{\sinh kd}$	1	0
Water particle velocity (y)	v	$\sigma\frac{\cosh kz}{\sinh kd}$	0	1
Water particle velocity (z)	w	$-i\sigma\frac{\sinh kz}{\sinh kd}$	0	0

k: wave number, σ: angular frequency, d: water depth, z: elevation from the bottom, ρ: fluid density, g: gravitational acceleration.

where the function h_m and the parameter α_m and β_m in Eq. (7) are the functions and the values as shown in Table 1[5)].

Equations (1) and (3) are the fundamental equations for the estimation of the directional spectrum on the bases of the simultaneous measurements of various wave properties. If the functions $S(\boldsymbol{k},\sigma)$ or $S(f,\theta)$ which satisfy Eq. (1) or Eq. (3) respectively and which take only non-negative values are obtained, the function is called a directional spectrum.

2.2 Existing methods for the estimation of directional spectrum

When an infinite number of wave properties are measured, *i.e.* the cross-power spectra are given for infinite pairs of m and n in Eq. (1) or (3), the directional spectrum can be uniquely estimated. However, in practice, only a limited number of wave properties are measured, and the directional spectrum cannot be determined uniquely. Therefore, several methods have been proposed to choose a single estimate of the directional spectrum.

(1) Direct Fourier Transformation Method (DFT)

This method is the fundamental approach and which gives the base for other method presently available. The method was first proposed by *Barber*[6)] for directional wave analysis utilizing an array of wave probes.

Rewriting Eq. (1) with the notation of the location vector $\boldsymbol{x}$ in place of $\boldsymbol{x}_n-\boldsymbol{x}_m$, and with the operation of the Fourier Inverse Transformation of Eq. (1), we obtain the following relationship:

$$S(\boldsymbol{k},\sigma)=\frac{1}{(2\pi)^2}\int_x \Phi(\boldsymbol{x},\sigma)\exp(i\boldsymbol{k}\boldsymbol{x})d\boldsymbol{x} \qquad (8)$$

In practice, the cross-power spectra are obtained only for a limited number of x, and the integration of Eq. (8) cannot be performed. *Barber* assumed that the values of the cross-power spectra be assigned zero at any distance x other than those realized by the measurement, and he proposed to use the following summation in place of Eq. (8).

$$\hat{S}(k,\sigma)=\alpha\sum_m\sum_n\Phi_{mn}(\sigma)\exp\{ik(x_n-x_m)\} \tag{9}$$

where α is a proportionality constant so that the estimate of the directional spectrum satisfies Eq. (6).

Equation (9) shows the estimate of the directional spectrum is expressed in a quadratic form and is rewritten in the form of a product of matrices as the following equation.

$$\hat{S}(k,\sigma)=\alpha D(k,\sigma)^{*t}\Phi(\sigma)D(k,\sigma) \tag{10}$$

where $D(k,\sigma)=\{\exp(ikx_1),\ldots\ldots,\exp(ikx_M)\}^t$, the superscript t denotes the transpose of a matrix, $\Phi(\sigma)$ is a $M\times M$ square matrix consisting of mn element being $\Phi_{mn}(\sigma)$, and is hermitian[#]. Equation (10) shows that the estimate of the directional spectrum $S(k,\sigma)$ is a real function, because it is expressed in a hermitian form of hermitian matrix.

When the hermitian matrix $\Phi(\sigma)$ is positive definite, the estimate of the directional spectrum $S(k,\sigma)$ is always greater than zero, and when it is positive semi-definite, $S(k,\sigma)$ is greater than or equal to zero.

The Direct Fourier Transformation Method is generally more stable than other methods to obtain the estimates of the directional spectrum, but the directional resolution is not high. In addition, the directional resolution and the stability of the estimates depends on the layout of the probe array. The optimum layout of the probe array is discussed by *Goda*[3].

Since this method computes the Fourier Inverse Transformation directly, and does not take into account the errors contained in the cross-power spectra, the stability and the reliability of the estimates depends on the accuracy of the cross-power spectra. If the probe array has an improper layout, errors contained in the cross-power spectra may result in an erroneous estimate of the directional spectrum.

A typical example of an improper array is illustrated in Fig. 1, where the sea state is supposed to be homogeneous over the sea area where the cross-power spectrum between the wave properties at point i and at point j should coincide with that between point k and point l. In practice, however, it is expected that the cross-power spectra measured from these two different pairs of wave probes give different values from each other because of the errors occurred in the measurement and in the computation of the cross-power spectra. Thus, the theoretical relationship between the true cross-power spectra and the true directional spectrum does not stand any more between the estimated cross-power spectra and the true directional spectrum.

(2) Extended Maximum Likelihood Method (EMLM)

The Extended Maximum Likelihood Method was proposed by *Isobe, et al.*[5], and the method is an expansion of the Maximum Likelihood Method developed by *Capon*[7] so that any combination of wave probes can be utilized for directional wave analysis.

[#] If a matrix is equal to its associate (or its transposed conjugate), *i.e.* $A=A^*$, the matrix is hermitian.

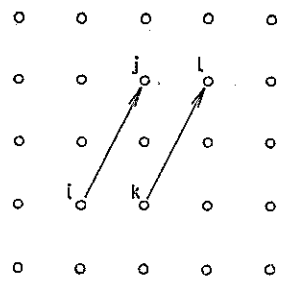

Fig. 1 Example of an improper layout of a wave probe array

The idea of the method is as follows.

Assuming the directional spectrum can be expressed by Eq. (11) as a linear superposition of the cross-power spectra on the analogy of Eq. (8).

$$\hat{S}(\boldsymbol{k}, \sigma)=\sum_m\sum_n \alpha_{mn}(\boldsymbol{k})\Phi_{mn}(\sigma) \tag{11}$$

Substituting the above equation into Eq. (1), we obtain the following equations:

$$\hat{S}(\boldsymbol{k}, \sigma)=\int_{\boldsymbol{k}'} S(\boldsymbol{k}', \sigma)w(\boldsymbol{k}, \boldsymbol{k}')d\boldsymbol{k}' \tag{12}$$

$$w(\boldsymbol{k}, \boldsymbol{k}')=\sum_m\sum_n \alpha_{mn}(\boldsymbol{k})H_m(\boldsymbol{k}', \sigma)H_n^*(\boldsymbol{k}', \sigma)\exp\{-i\boldsymbol{k}'(\boldsymbol{x}_n-\boldsymbol{x}_m)\} \tag{13}$$

Equations (12) and (13) show that the estimate of the directional spectrum is a convolution of the true directional spectrum and a window function $w(\boldsymbol{k}, \boldsymbol{k}')$. Therefore, the closer the window function $w(\boldsymbol{k}, \boldsymbol{k}')$ to the delta function, the closer the estimate reaches the true directional spectrum. After some manipulation of above mentioned window function, *Isobe* proposed the following formula to estimate the directional spectrum.

$$\hat{S}(\boldsymbol{k}, \sigma)=\kappa/[\sum_m\sum_n \Phi_{mn}^{-1}(\sigma)H_m^*(\boldsymbol{k}, \sigma)H_n(\boldsymbol{k}, \sigma)\exp\{i\boldsymbol{k}(\boldsymbol{x}_n-\boldsymbol{x}_m)\}] \tag{14}$$

where $\Phi_{mn}^{-1}(\sigma)$ is the mn element of the inverse matrix $\boldsymbol{\Phi}^{-1}(\sigma)$ of $\boldsymbol{\Phi}(\sigma)$, and κ is a proportionality constant which is determined so that the estimate of the directional function $S(\boldsymbol{k}, \sigma)$ satisfies Eq. (6).

The EMLM is said to have a high directional resolution and versatility, and has been widely employed in the directional wave analysis.

The above Eq. (14) can be rewritten in a matrix expression as follows.

$$\hat{S}(\boldsymbol{k}, \sigma)=\frac{\kappa}{\boldsymbol{D}(\boldsymbol{k}, \sigma)^{*t}\boldsymbol{\Phi}^{-1}(\sigma)\boldsymbol{D}(\boldsymbol{k}, \sigma)} \tag{15}$$

where, $\boldsymbol{D}(\boldsymbol{k}, \sigma)=\{H_1(\boldsymbol{k}, \sigma)\exp(i\boldsymbol{k}\boldsymbol{x}_1), \ldots, H_M(\boldsymbol{k}, \sigma)\exp(i\boldsymbol{k}\boldsymbol{x}_M)\}^t$, and $\boldsymbol{\Phi}^{-1}(\sigma)$ is the inverse matrix of $\boldsymbol{\Phi}(\sigma)$.

If $\boldsymbol{A}$ is a hermitian matrix, the expression $\boldsymbol{X}^{*t}\boldsymbol{A}\boldsymbol{X}$ is known as a hermitian form.

As seen in Eq. (15), the estimate of the directional spectrum is given by a function having a denominator given in a hermitian form#. Therefore, the estimate of the directional spectrum $S(\boldsymbol{k}, \sigma)$ is real, since the matrix $\boldsymbol{\Phi}^{-1}(\sigma)$ is hermitian. The estimate of $S(\boldsymbol{k}, \sigma)$ takes non-negative and finite values only if the matrix $\boldsymbol{\Phi}^{-1}(\sigma)$ is positive definite. In case the matrix $\boldsymbol{\Phi}^{-1}(\sigma)$ is not positive definite, the directional spectrum $S(\boldsymbol{k}, \sigma)$ may result in negative or infinite values.

In addition, since the directional spectrum given by the EMLM is expressed as a reciprocal of the function expressed in a quadratic form, the spectral peak appears at the direction where the denominator takes a minimum value which may be very close to zero, while the denominator takes very large value for the direction where the spectral density is zero. Thus the peak value of the directional spectrum is very vulnerable to the truncation error in the computation, and the values of the directional spreading function are sometimes overestimated for the directions where the spectral density is close to zero. This might often lead to an ill-conditioned shape for the resulting estimate of the directional spectrum.

Furthermore, when the cross-power spectra are contaminated with errors, matrix $\boldsymbol{\Phi}(\sigma)$ is not always positive definite, *Jefferies*[8] proposed to modify the matrix by adding a certain constant value to the elements of it. However, this technique is just for the purpose of convenience, and it does not give a solution to the essential problem.

It is seen that one of the causes why those problems mentioned above happen is the utilization of Eq. (11) in place of Eq. (8). The relationship between the cross-power spectra and the directional spectrum expressed by Eq. (8), *i.e.* the Fourier Inverse Transformation of the cross-power spectra is equal to the directional spectrum, is mathematically valid. However, this does not guarantee the validity of Eq. (11), since the summation is truncated for finite numbers of m and n. It is sometimes true that simple mathematical manipulation misleads the proper recognition of complicated actual physical phenomena.

As described for the DFT, the EMLM neither takes into account the errors associated with the cross-power spectra, and may therefore yield erroneous estimates of the directional spectrum when the layout of the probe array is not proper.

(3) The Maximum Entropy Principle Method (MEP)

This method was proposed by the authors[9], and is a powerful method for estimating the directional spectrum for a point measurement of three elements of the wave properties, such as a discus buoy or a two axis directional current meter with a wave gauge. The following is the brief explanation of the method.

The directional spreading function $G(\theta|f)$ is defined within the directional range $[0, 2\pi]$, and does not take negative values. It also satisfies Eq. (5), *i.e.* the definite integral of $G(\theta|f)$ over the full directional range from 0 to 2π is equal to 1.0. These restrictions imposed on the directional spreading function are the same as those imposed on probability density functions which are often utilized to describe the statistical characteristics of random variables. Thus, it is expected that the directional spreading functions can be estimated through the same procedure as when the probability density function is determined.

One of the popular approaches is to choose the probability density function which maximizes the entropy. The information entropy which is called the *Shannon's entropy* is defined by Eq. (16).

$$H=-\int_0^{2\pi} G(\theta|f)\ln G(\theta|f)d\theta \tag{16}$$

The estimate of the directional spreading function $G(\theta|f)$ which maximizes the entropy H under the restriction condition given by Eq. (3) is called the maximum entropy estimate. In consequence, the estimate for the case of three-element measurements is given by Eq. (17)[9].

$$\hat{G}(\theta|f)=\exp\{-\lambda_0-\lambda_1\cos\theta-\lambda_2\sin\theta-\lambda_3\cos 2\theta-\lambda_4\sin 2\theta\} \tag{17}$$

where the coefficients $\lambda_0,\ldots,\lambda_4$ are the *Lagrange's* multipliers which are determined by nonlinear equations so that the estimate satisfies the restriction conditions Eq. (3).

As mentioned later, both of the MEP and the EMLM approximate the directional spreading function by certain models. The former employs an exponential function of which power is expressed in series, while the later utilizes a reciprocal of a function expressed in a quadratic form. The advantage of the former over the latter is that the model utilized does not take negative values, which well reflect the nature of the directional spreading function.

For the cases of three-element measurements, the nonlinear equations can be solved relatively easily by numerical iteration. On the other hand, when the wave properties more than 4 elements (which is called multi-element measurement hereafter) are employed in the directional wave analysis, the iteration failed to yield the values of unknown *Lagrange's* multipliers.

By improving the scheme of the iteration computation to solve nonlinear equations, it may be expected that the MEP successfully yields the values of the unknown coefficients even for the latter case. The authors suspect that the failure of the method results not from merely the scheme of the computation but from the inherent demerits of the basic principle of the method.

The formulation of the MEP method is based on the hypothesis that the maximum entropy estimate exists and that it exactly satisfies the restriction condition. Therefore, if the mathematical relationship between the directional spectrum and the cross-power spectra is destroyed in the multi-element measurement by errors contained in the estimates of the cross-power spectra, the method fails to find the maximum entropy estimate. Hence, depending on the layout of the probe array and the errors contained in the cross-power spectra, the solution of the maximum entropy estimate may not exist. Unless the contradiction between the cross-power spectra is removed, the MEP can not be employed to analyze multi-element measurement.

(4) Discussion on entropy

Akaike[10),11)] pointed out that there had been the misunderstanding of the entropy defined by Eq. (16), whch is known as *Shannon's entropy*, and gave an explanation to the essential form of the entropy proposed by *Boltzmann*. He formulated the Entropy $B(p:q)$ as Eq. (18),

$$B(p:q)=-\int p(x)\ln p(x)dx+\int p(x)\ln q(x)dx \tag{18}$$

According to *Akaike*, the function $p(x)$ in the right hand side of Eq. (18) corresponds to the true probability density function of a phenomenon (which is called the true distribution hereafter), and the function $q(x)$ corresponds to the probability density function which is introduced to describe the statistical charac-

teristics of the phenomenon (which is called the model distribution hereafter). Thus, *Boltzmann's entropy* $B(p:q)$ interpreted as the logarithm of the probability that the true distribution $p(x)$ is obtained from the model distribution $q(x)$ when the true distribution belongs to the family of the model distribution $q(x)$. Hence, he commented that $B(p:q)$ is quite a reasonable criterion to indicate the degree of the approximation of the true distribution $p(x)$ by the model distribution $q(x)$.

Boltzmann's entropy has such characteristics as given by Eq. (19).

$$\left.\begin{array}{ll} \text{(i)} & B(p:q)<0 : p(x)\neq q(x) \\ \text{(ii)} & B(p:q)=0 : p(x)=q(x) \end{array}\right\} \tag{19}$$

Equation (19) shows that the *Boltzmann's entropy* $B(p:q)$ takes maximum value 0 when the model distribution $q(x)$ is identical to the true distribution $p(x)$.

When a uniform probability density function is employed as the model distribution $q(x)$ in Eq. (18), the *Boltzmann's entropy* is formally identical to the *Shannon's entropy*, which is utilized by the MEP as a criterion to indicate the degree of fitness. Therefore, it can be said that the MEP chooses a directional spreading function which is the closest to the uniform distribution among various candidates for the function. This seems to be another advantage of the MEP, because the uniform distribution is the simplest energy distribution and the energy distribution observed in many natural phenomena is expected to be a simple one. Because of the tendency of the MEP to choose the simplest distribution, it estimates the directional spreading function on the basis of only the essential information provided by the cross-power spectra without being affected by other inessential ones.

However, from the viewpoint of the entropy, the MEP does not manipulate the model distribution, but manipulate the true distribution in order that the true distribution becomes closer to the uniform distribution. This approach is reverse way of the essential approach of the maximum entropy principle.

(5) Underlying problems of the existing estimation methods

From the review of the three kinds of existing methods for the estimation of the directional spectrum, especially from the viewpoint of the problems inherent to each method, it is found that all the three methods formulate their own models of approximating functions which are characterized by some unknown parameters, and that they set up the same number of equations as the number of the unknown parameters of their respective models. Though the principles and the methods of deriving the models are different, all of these methods try to fit their respective parametric models to the relation with the given cross-power spectra. The advantage and the disadvantage of these methods therefore results from the characteristics of the models utilized by each method.

Directional wave analysis has the problem of estimating the various characteristics of the directional wave from only a limited amount of the information and there are many unknown elements which cannot determined by the given information. The presently available methods make much use of the mathematical approach and successfully estimate the directional spectrum with the help of the models characterized by as many parameters as can be determined by the information.

However, as far as we rely on the formal mathematical approach, we may end up with results far from the real phenomena. In fact, there are hidden pitfalls in the existing methods, as illustrated in the earlier part of this section. It should be

noted that the realized wave data are samples of the population, and that the all the existing methods try to estimate the directional spectrum on the basis of only realized data.

Thus, it is inevitable for existing methods to utilize formal mathematical manipulation and that such models be characterized by few parameters. These mathematical models are able to approximate the real directional spectrum only if the real spectrum is suitable to fit the model.

Therefore, for the discussion on the real directional spectrum, considering the inherent nature of the phenomenon of interest, we have to set up flexible models that have a higher degree of freedom and that have the underlying nature of ocean random waves inherent.

3. Estimation of Directional Spectrum from the Bayesian Approach

3.1 Basic principle of the Bayesian approach[11),13)]

In this section, the principle of the Bayesian approach in the field of statistics, is reviewed briefly.

One of the basic theorems related to probability is *Bayes' theorem*, which expresses the relationship between the joint probability density function and the conditional probability density function.

$$p(x, y)=p(x|y)p(y)=p(y|x)p(x) \tag{20}$$

Equation (20) is rewritten in the following form.

$$p(y|x)=\frac{p(x|y)p(y)}{p(x)} \tag{21}$$

The above equation is a useful relationship for estimating the random variable y on the bases of given sample data x. If x and y are regarded as the sample data and the parameter of the conditional probability density function $p(x \mid y)$ respectively, $p(x \mid y)$ is called the model distribution, and $p(y)$ and $p(y \mid x)$ are called the prior distribution and the posterior distribution respectively. The prior distribution $p(y)$ reflects the statistical nature of a phenomenon which we assume a priori and without the information given by the data, and the posterior distribution $p(y \mid x)$ reflects both of the a priori condition $p(y)$ and the statistical characteristics of the model distribution $p(x \mid y)$[13)].

When the sample data x are known and the model distribution $p(x \mid y)$ is considered as a function of the parameter y, $p(x \mid y)$ is called the likelihood function $L(y \mid x)$ expressing the likelihood of y. Equation (21) implies the following relationship with respect to y for the given realized sample data x.

$$p(y|x) \propto L(y|x)p(y) \tag{22}$$

i.e.,

$$\text{(Posterior distribution)} \propto \text{(likelihood)} \times \text{(Prior distribution)} \tag{23}$$

This relationship gives the essential relation which is the base of the Bayesian approach in the estimation of the parameter of the model distribution.

For the practical application of Eq. (22) to the estimation of the parameter y

under the given model distribution $p(x \mid y)$, it is necessary to give the prior distribution $p(y)$. Since the prior distribution is not given uniquely in general, the Bayesian approach had not been employed in the statistical analysis for many years.

Incidentally, the maximum likelihood method, which is commonly employed at present, is the method on the basis of the likelihood function only with the assumption that the prior distribution to be uniform distribution *i.e.* $p(y)=1/I$ in Eq. (22)[11].

3.2 Bayesian approach for regression analysis[14)-19)]

The Bayesian approach is originally introduced by *Akaike*[1] as a tool to deal with a regression analysis problem where the number of the parameters to be estimated is large compared with the sample size. The following is the brief review of the Bayesian approach to estimate regression coefficients given by *Ishiguro and Sakamoto*[15].

Assume that the variable y is expressed by a linear regression of a vector of independent variable $\boldsymbol{x}$ as given by Eq. (24).

$$y=\boldsymbol{x}^t\boldsymbol{\alpha}+\varepsilon \tag{24}$$

where $\boldsymbol{\alpha}$ is the vector of unknown coefficients and ε is a random variable of which occurrence follows the normal distribution having a mean 0 and a variance σ^2.

For a given set of sample data $(y_i, \boldsymbol{x}_i)$, $(i=1, \ldots\ldots, n)$, the maximum likelihood estimate is the one which minimize the value of Eq. (25).

$$\sum_{i=1}^{n} |y_i-\boldsymbol{x}_i{}^t\boldsymbol{\alpha}|^2=|\boldsymbol{y}-\boldsymbol{X}\boldsymbol{\alpha}|^2 \tag{25}$$

where $\boldsymbol{y}=(y_1, \ldots\ldots, y_n)^t$, $\boldsymbol{X}=(\boldsymbol{x}_1, \ldots\ldots, \boldsymbol{x}_n)^t$.

When the regression model is chosen from a family which are characterized by a relatively low order of unknown coefficient vector, *i.e.* not greater than $2\sqrt{n}$, a suitable model can be selected with the use of the MAICE (Minimum AIC Estimation) method[19] on the basis of the AIC (*Akaike's Information Criterion*)[20].

However, when the number of data n is less than the order of unknown coefficient vector $\boldsymbol{\alpha}$, the model becomes unstable or the coefficients sometimes cannot be determined by Eq. (25).

For this case, taking into account the balance of the suitability of the model and the smoothness of the model, and assuming that $\boldsymbol{\alpha}$ is close to known value $\boldsymbol{\alpha}_0$ or, for a certain matrix $\boldsymbol{D}$, $|\boldsymbol{D}(\boldsymbol{\alpha}-\boldsymbol{\alpha}_0)|^2$ is small enough, the estimate of unknown coefficients are determined as the vector which minimizes Eq. (26).

$$|\boldsymbol{y}-\boldsymbol{X}\boldsymbol{\alpha}|^2+u^2|\boldsymbol{D}(\boldsymbol{\alpha}-\boldsymbol{\alpha}_0)|^2 \tag{26}$$

The estimate which minimizes Eq. (26) varies depending on the values of the parameter u, and thus, how to give the value u is the next problem.

Akaike solved this problem by considering that to minimize Eq. (26) is to maximize Eq. (27),

$$\exp\left\{-\frac{1}{2\sigma^2}|\boldsymbol{y}-\boldsymbol{X}\boldsymbol{\alpha}|^2\right\}\exp\left\{-\frac{u^2}{2\sigma^2}|\boldsymbol{D}(\boldsymbol{\alpha}-\boldsymbol{\alpha}_0)|^2\right\} \tag{27}$$

The first term of Eq. (27) is proportional to the likelihood $L(\boldsymbol{\alpha}, \sigma^2|\boldsymbol{y})$ of $\boldsymbol{\alpha}$ and σ^2 for the given data set $(y_i, \boldsymbol{x}_i)$, $(i=1, \ldots\ldots, n)$, and the second term is the prior

distribution $p(\boldsymbol{a}|u^2, \sigma^2)$ of $\boldsymbol{a}$. Therefore, the posterior distribution of $\boldsymbol{a}$ is proportional to the product of the likelihood of the model and the prior distribution (see Eq. (22)), and hence the estimate given as the vector minimizing Eq. (26) should be the mode of the posterior distribution. In addition, u^2 in Eq. (27) is a sort of the weighting constant (which is called the Hyperparameter) characterizing a prior distribution of $\boldsymbol{a}$. So, the choice of u is interpreted as that of a parameter of prior distribution of $\boldsymbol{a}$. Form these considerations, *Akaike* proposed the use of the marginal likelihood given by

$$\int L(\boldsymbol{a}, \sigma^2|\boldsymbol{y})p(\boldsymbol{a}|u^2, \sigma^2)d\boldsymbol{a} \tag{28}$$

as a criterion for the choice of u^2 and σ^2. Those values are to be chosen so that Eq. (28) is maximized. Considering the relation to the statistic AIC, *Akaike* defined the statistic ABIC (*Akaike's Bayesian Information Criterion*) by

$$\text{ABIC}=-2\ln\int L(\boldsymbol{a}, \sigma^2|\boldsymbol{y})p(\boldsymbol{a}|u^2, \sigma^2)d\boldsymbol{a} \tag{29}$$

The value of u^2 and σ^2 is to be chosen so that it minimizes ABIC.

3.3 Formulation of the directional spectral estimation from the Bayesian Approach

To simplify the nomenclature of the terms in the equations, Eq. (3) is rewritten in the following form using the upper triangular components of the hermitian matrix $\boldsymbol{\Phi}(\sigma)$.

$$\phi_i(f)=\int_0^{2\pi} H_i(f, \theta)G(\theta|f)d\theta \qquad (i=1, \cdots, N) \tag{30}$$

where,

$$N=M\times(M+1)/2\,; \quad M: \text{Number of the wave probes} \tag{31}$$

$$H_i(f, \theta)=H_m(f, \theta)H_n^*(f, \theta)[\cos\{k(x_{mn}\cos\theta+y_{mn}\sin\theta) - i\sin\{k(x_{mn}\cos\theta+y_{mn}\sin\theta)\}]/\sqrt{\Phi_{mm}(f)\Phi_{nn}(f)} \tag{32}$$

$$\phi_i(f)=\Phi_{mn}(f)/\{S(f)\sqrt{\Phi_{mm}(f)\Phi_{nn}(f)}\} \tag{33}$$

$$G(\theta|f)=S(f, \theta)/S(f) \tag{34}$$

The directional spreading function takes values greater than or equal to zero, but in this section, the function is treated as a function which always takes positive values only.

Firstly, it is assumed that the directional spreading function is expressed as a piecewise-constant function over the directional range from 0 to 2π ($K\Delta\theta=2\pi$). This assumption is commonly employed in the numerical computation of random waves.

Since $G(\theta|f)>0$, and let

$$\ln G(\theta_k|f)=x_k(f), \quad (k=1\cdots\cdots, K) \tag{35}$$

the directional spreading function is approximated by the following equation.

$$G(\theta|f)\doteqdot\sum_{k=1}^{K}\exp\{x_k(f)\}I_k(\theta) \tag{36}$$

where,

$$I_k(\theta)=\begin{cases}1 : (k-1)\Delta\theta\leq\theta<k\Delta\theta \\ 0 : \text{otherwise}, \quad (k=1\cdots\cdots, K)\end{cases} \tag{37}$$

Substituting Eq. (36) into Eq. (30), the following equation is obtained.

$$\phi_i(f)=\sum_{k=1}^{K}\exp\{x_k(f)\}\int_0^{2\pi}H_i(f,\theta)I_k(\theta)d\theta \tag{38}$$

When the value K is large enough, the integral of the right hand side of Eq. (38) is further approximated by Eq. (39).

$$\int_0^{2\pi}H_i(f,\theta)I_k(\theta)d\theta=\int_{(k-1)\Delta\theta}^{k\Delta\theta}H_i(f,\theta)I_k(\theta)d\theta\fallingdotseq H_i(f,\theta_k)\Delta\theta\equiv\alpha_{ik}(f) \tag{39}$$

For the convenience of the expression of the equations, the complex numbers ϕ_i and $\alpha_{i,k}$ are written in the following forms,

$$\left.\begin{aligned}\phi_i&=\text{Real}\{\phi_i(f)\}\\ \phi_{N+i}&=\text{Imag}\{\phi_i(f)\}\\ \alpha_{i,k}&=\text{Real}\{\alpha_{i,k}(f)\}\\ \alpha_{N+i,k}&=\text{Imag}\{\alpha_{i,k}(f)\}\end{aligned}\right\} \tag{40}$$

so that ϕ_i and $\alpha_{i,k}$ $(i=1,\ldots\ldots,2N)$ are real numbers. In Eq. (40), though the left hand sides are the functions of the frequency f, f is omitted to simplify the expression. Equation (38) is then expressed as Eq. (41).

$$\phi_i=\sum_{k=1}^{K}\alpha_{i,k}\exp(x_k)\qquad(i=1,\cdots\cdots,2N) \tag{41}$$

When the relation (Eq. (41)) is applied to the observed data, the error contained in the data must be taken into account and so Eq. (41) is modified to Eq. (42) in consideration of the existence of the errors.

$$\phi_i=\sum_{k=1}^{K}\alpha_{i,k}\exp(x_k)+\varepsilon_i\qquad(i=1,\cdots\cdots,2N) \tag{42}$$

where ε_i $(i=1,\ldots\ldots,2N)$ are independent from each other, and the probability of their occurrence is expressed by the normal distribution having the mean 0 and the variance σ^2.

For the given ϕ_i $(i=1,\ldots\ldots,2N)$, the likelihood function of x_k; $(k=1,\ldots\ldots,K)$ and σ^2 is given by Eq. (43).

$$L(x_1,\cdots\cdots,x_K\,;\,\sigma^2)=\frac{1}{(2\pi\sigma^2)^N}\exp\left[-\frac{1}{2\sigma^2}\sum_{i=1}^{2N}\left\{\phi_i-\sum_{k=1}^{K}\alpha_{i,k}\exp(x_k)\right\}^2\right] \tag{43}$$

In the derivation of the equations mentioned above, the directional spreading function $G(\theta|f)$ is expressed by a piecewise constant function. However, so far, the correlation between the wave energy falling on each segment of θ has not yet taken into account. Since the directional wave analysis is based on the linear wave theory, it can be assumed that the energy falls on each segment of the wave direction is independent from each other, but it is not real to assume that the energy distribution over the wave directions is not continuous. In general, the directional spreading

function can be supposed to be a continuous and smooth function.

Therefore, the additional condition that the variation of x_k; $(k=1, \ldots\ldots, K)$ should be locally well-approximated by a linear function, which is the mathematical expression of the continuity and the smoothness of the directional spreading function. Introducing this condition, the second derivative of $\ln G(\theta \mid f)$ *i.e.* the differences of the second order of $\{x_k\}$ is characterized by the following equation,

$$x_k - 2x_{k-1} + x_{k-2} \fallingdotseq 0 \tag{44}$$

This leads to the condition that

$$\sum_{k=1}^{K} \{x_k - 2x_{k-1} + x_{k-2}\}^2 \qquad (x_0 = x_K, x_{-1} = x_{K-1}) \tag{45}$$

becomes smaller as the estimate of the directional spreading function $G(\theta \mid f)$ becomes smoother.

Therefore, it is supposed that the estimate of the directional spreading function is the one which maximizes the likelihood (Eq. (43)) and which minimizes Eq. (45) at the same time. The procedure to find the estimate is formulated as follows.

The most suitable estimate of the directional spreading function is given as a set of x_k which maximizes Eq. (46) for a given hyperparameter u^2.

$$\ln L(x_1, \cdots\cdots, x_K\,;\, \sigma^2) - \frac{u^2}{2\sigma^2} \sum_{k=1}^{K} (x_k - 2x_{k-1} + x_{k-2})^2 \tag{46}$$

The maximization of Eq. (46) is achieved by maximizing the exponential function having the power expressed by Eq. (46). This leads to the maximization of Eq. (47).

$$L(x_1, \cdots\cdots, x_K\,;\, \sigma^2) \exp\left\{ -\frac{u^2}{2\sigma^2} \sum_{k=1}^{K} (x_k - 2x_{k-1} + x_{k-2})^2 \right\} \tag{47}$$

Incidentally, Eq. (47) corresponds to the right hand side of Eq. (22), provided that the prior distribution of $\boldsymbol{x} = (x_1, \ldots\ldots, x_K)$ is given by Eq. (48).

$$p(\boldsymbol{x} \mid u^2, \sigma^2) = \left(\frac{u}{\sqrt{2\pi}\sigma} \right)^K \exp\left\{ -\frac{u^2}{2\sigma^2} \sum_{k=1}^{K} (x_k - 2x_{k-1} + x_{k-2})^2 \right\} \tag{48}$$

For a given set of observed data, the posterior distribution $p_{\mathrm{post}}(\boldsymbol{x} \mid u^2, \sigma^2)$ is proportional to the likelihood $L(\boldsymbol{x}, \sigma^2)$ and the prior distribution $p(\boldsymbol{x} \mid u^2, \sigma^2)$, that is

$$p_{\mathrm{post}}(\boldsymbol{x} \mid u^2, \sigma^2) \propto L(\boldsymbol{x}, \sigma^2) p(\boldsymbol{x} \mid u^2, \sigma^2) \tag{49}$$

Thus, the estimate of $\boldsymbol{x}$ obtained by maximizing Eq. (49) is regarded as the mode of the posterior distribution of $p_{\mathrm{post}}(\boldsymbol{x} \mid u^2, \sigma^2)$.

If the value of u is given, the value of $\boldsymbol{x}$ which maximizes Eq. (49) are determined by minimizing Eq. (50), regardless of the values of σ^2.

$$\sum_{i=1}^{2N} \left\{ \phi_i - \sum_{k=1}^{K} \alpha_{i,k} \exp(x_k) \right\}^2 + u^2 \left\{ \sum_{k=1}^{K} (x_k - 2x_{k-1} + x_{k-2})^2 \right\} \tag{50}$$

The most suitable values of the hyperparameter u^2 and the variance σ^2 are determined so that the ABIC is minimum.

$$\mathrm{ABIC} = -2 \ln \int L(\boldsymbol{x}, \sigma^2) p(\boldsymbol{x} \mid u^2, \sigma^2) d\boldsymbol{x} \tag{51}$$

3.4 Numerical computation of the directional spectrum

In order to estimate the directional spectrum by means of the Bayesian approach, the minimization of Eq. (50) and the integration and the minimization of Eq. (51) must be performed. The following is the procedure of the computation utilized by *Ishiguro* [18] and *Sakamoto*[14].

With the use of matrix expression, Eq. (50) is written in the form of Eq. (52),

$$J(\boldsymbol{x})=|\boldsymbol{AF}(\boldsymbol{x})-\boldsymbol{B}|^2+u^2|\boldsymbol{Dx}|^2 \tag{52}$$

where,

$$\boldsymbol{A}=\begin{bmatrix} \alpha_{1,1}, \cdots\cdots, \alpha_{1,K} \\ \vdots \quad \ddots \\ \alpha_{2N,1}, \cdots, \alpha_{2N,K} \end{bmatrix} \tag{53}$$

$$\boldsymbol{B}=(\phi_1, \cdots\cdots, \phi_{2N})^t \tag{54}$$

$$\boldsymbol{F}(x)=\{\exp(x_1), \cdots\cdots, \exp(x_K)\}^t \tag{55}$$

$$\boldsymbol{D}=\begin{bmatrix} 1 & 0 & 0\cdots\cdots 0 & 1 & -2 \\ -2 & 1 & 0\cdots\cdots 0 & 0 & 1 \\ 1 & -2 & 1\cdots\cdots 0 & 0 & 0 \\ \vdots & \vdots & \vdots \quad \ddots & \vdots & \vdots \\ 0 & 0 & 0\cdots\cdots 1 & -2 & 1 \end{bmatrix} \tag{56}$$

The first term of the right hand side of Eq. (52) is nonlinear with respect to $\boldsymbol{x}$, and it is linearized by utilizing the Taylor expansion of $\boldsymbol{F}(\boldsymbol{x})$ about $\boldsymbol{x}_0$, which is a value close to the estimate of $\boldsymbol{x}$,

$$\boldsymbol{F}(\boldsymbol{x})\fallingdotseq\boldsymbol{F}(\boldsymbol{x}_0)+\boldsymbol{E}(\boldsymbol{x}_0)(\boldsymbol{x}-\boldsymbol{x}_0) \tag{57}$$

where,

$$\boldsymbol{E}(\boldsymbol{x})=\begin{bmatrix} -\exp(x_1) & 0 & \cdots\cdots & 0 \\ 0 & \exp(x_2) & \cdots\cdots & 0 \\ \vdots & \vdots & \ddots & \vdots \\ 0 & 0 & \cdots\cdots & \exp(x_K) \end{bmatrix} \tag{58}$$

Substituting Eq. (57) into Eq. (52), we obtain the following equation after some rearrangement of the equation,

$$J(\boldsymbol{x})\cong|\tilde{\boldsymbol{A}}\boldsymbol{x}-\tilde{\boldsymbol{B}}|^2+u^2|\boldsymbol{Dx}|^2 \tag{59}$$

where,

$$\tilde{\boldsymbol{A}}=\boldsymbol{AE}(\boldsymbol{x}_0) \tag{60}$$

$$\tilde{B}=B-AF(x_0)+AE(x_0)x_0 \tag{61}$$

Thus, for a certain initial value x_0, the values of x_1 are computed by means of the least square method utilizing Eq. (59) through Eq. (61). Substituting these x_1 for the initial value x_0 in Eq. (59) to Eq. (61), and repeating the same process, we obtain the another set of x_2. Iterating these process until the values of x converges to $\hat{x}$, the estimate of x is obtained for the given value of u^2. In the practical computation of the least square method, the Householder method[19], is employed. The procedure is as follows.

Equation (59) is rewritten as

$$J(x)=\left|\begin{pmatrix}\tilde{A}\\ uD\end{pmatrix}x-\begin{pmatrix}\tilde{B}\\ O\end{pmatrix}\right|^2 \tag{62}$$

Therefore, letting

$$Z=\left(\begin{array}{c|c} \tilde{A} & \tilde{B} \\ \hline uD & O \end{array}\right)\begin{matrix}\uparrow\\ 2N\\ \downarrow\\ \uparrow\\ K\\ \downarrow\end{matrix}\quad \begin{matrix}|\leftarrow K\rightarrow| & |\leftarrow 1\rightarrow|\end{matrix}, \tag{63}$$

the Householder transformation (the transformation of an arbitrary matrix to upper triangular matrix by repeating the mirror image transformation) can be performed. The matrix computation of mirror image transformation is expressed by the following equations.

$$U=I-2ww^t \tag{64}$$

$$w=\frac{a-b}{|a-b|} \tag{65}$$

where I denotes the unit matrix, a is an arbitrary vector, and b is the vector obtained by the mirror image transformation of vector a.

If the matrix

$$UZ=\begin{bmatrix} S_{1,1} & \cdots & S_{1,K+1} \\ & \ddots & \vdots \\ & & S_{K+1,K+1} \\ & O & \end{bmatrix} \tag{66}$$

is obtained by the Householder transformation, then Eq. (62) is rewritten as

$$\left|U\begin{pmatrix}\tilde{A}\\ uD\end{pmatrix}x-U\begin{pmatrix}\tilde{B}\\ O\end{pmatrix}\right|^2=\left|\begin{pmatrix}S_{1,1} & \cdots & S_{1,K}\\ & \ddots & \vdots\\ O & & S_{KK}\end{pmatrix}\begin{pmatrix}x_1\\ \vdots\\ x_K\end{pmatrix}-\begin{pmatrix}S_{1,K+1}\\ \vdots\\ S_{K+1,K+1}\end{pmatrix}\right|^2$$

$$=\left|\begin{pmatrix}S_{1,1} & \cdots & S_{1,K}\\ & \ddots & \vdots\\ O & & S_{K,K}\end{pmatrix}\begin{pmatrix}x_1\\ \vdots\\ x_K\end{pmatrix}-\begin{pmatrix}S_{1,K+1}\\ \vdots\\ S_{K,K+1}\end{pmatrix}\right|+S^2_{K+1,K+1} \tag{67}$$

Since the second term of the right hand side of Eq. (67) is independent from x, the

least square estimate of x which minimizes Eq. (59) or (62) is obtained by solving Eq. (68).

$$\begin{pmatrix} S_{1,1} & \cdots & S_{1,K} \\ & \ddots & \vdots \\ \boldsymbol{O} & & S_{K,K} \end{pmatrix} \begin{pmatrix} x_1 \\ \vdots \\ x_K \end{pmatrix} = \begin{pmatrix} S_{1,K+1} \\ \vdots \\ S_{K,K+1} \end{pmatrix} \tag{68}$$

The variance of the residual is calculated by

$$S^2_{K+1,K+1}/(2N) \tag{69}$$

Since the estimates of x are computed through the above mentioned procedure, the next step is to calculate the ABIC (Eq. (51)) and the Variance σ^2 in Eq. (43). The method of computation is as follows.

During the process of the computation of x, the coefficient matrix $\boldsymbol{A}$ and $\boldsymbol{B}$ are renewed at each iteration. Let $\hat{\boldsymbol{A}}$ and $\hat{\boldsymbol{B}}$ are the coefficient matrix which are computed for the least square estimate $\hat{x}$. Then, the posterior distribution is proportional to Eq. (70).

$$\begin{aligned} &L(x, \sigma^2)p(x|u^2, \sigma^2) \\ &\doteqdot \left(\frac{1}{2\pi\sigma^2}\right)^N \exp\left\{-\frac{1}{2\sigma^2}|\hat{\boldsymbol{A}}x-\hat{\boldsymbol{B}}|^2\right\}\left(\frac{u}{\sqrt{2\pi}\sigma}\right)^K \exp\left\{-\frac{u^2}{2\sigma^2}|\boldsymbol{D}x|^2\right\} \\ &= \left(\frac{1}{2\pi\sigma^2}\right)^N \left(\frac{u}{\sqrt{2\pi}\sigma}\right)^K \exp\left\{-\frac{1}{2\sigma^2}\left|\begin{pmatrix}\hat{\boldsymbol{A}}\\ u\boldsymbol{D}\end{pmatrix}\hat{x}-\begin{pmatrix}\hat{\boldsymbol{B}}\\ \boldsymbol{O}\end{pmatrix}\right|^2\right\} \exp\left\{-\frac{1}{2\sigma^2}\left|\begin{pmatrix}\hat{\boldsymbol{A}}\\ u\boldsymbol{D}\end{pmatrix}(x-\hat{x})\right|^2\right\} \end{aligned} \tag{70}$$

Therefore, the integration of Eq. (70) is given as

$$\begin{aligned} &\int_{-\infty}^{\infty} L(x, \sigma^2)p(x|u^2, \sigma^2)dx \\ &= \left(\frac{1}{2\pi\sigma^2}\right)^N \left(\frac{u}{\sqrt{2\pi}\sigma}\right)^K \exp\left\{-\frac{1}{2\sigma^2}\left|\begin{pmatrix}\hat{\boldsymbol{A}}\\ u\boldsymbol{D}\end{pmatrix}\hat{x}-\begin{pmatrix}\hat{\boldsymbol{B}}\\ \boldsymbol{O}\end{pmatrix}\right|^2\right\} \\ &\quad \times \int_{-\infty}^{\infty} \exp\left\{-\frac{1}{2\sigma^2}\left|\begin{pmatrix}\hat{\boldsymbol{A}}\\ u\boldsymbol{D}\end{pmatrix}(x-\hat{x})\right|^2\right\}dx \end{aligned} \tag{71}$$

From the integration formula, the second term of the right hand side of Eq. (71) is written in the form of Eq. (72).

$$\int_{-\infty}^{\infty} \exp\left\{-\frac{1}{2\sigma^2}\left|\begin{pmatrix}\hat{\boldsymbol{A}}\\ u\boldsymbol{D}\end{pmatrix}(x-\hat{x})\right|^2\right\}dx = (\sqrt{2\pi}\sigma)^K \{\det(\hat{\boldsymbol{A}}^t\hat{\boldsymbol{A}}+u^2\boldsymbol{D}^t\boldsymbol{D})\}^{-1/2} \tag{72}$$

Thus, Eq. (71) is rewritten as follows.

$$\begin{aligned} &\int_{-\infty}^{\infty} L(x, \sigma^2)p(x|\sigma^2, u^2)dx \\ &= \left(\frac{1}{2\pi\sigma^2}\right)^N u^K \exp\left[-\frac{1}{2\sigma^2}\{|\hat{\boldsymbol{A}}\hat{x}-\hat{\boldsymbol{B}}|^2+u^2|\boldsymbol{D}\hat{x}|^2\}\right]\{\det(\hat{\boldsymbol{A}}^t\hat{\boldsymbol{A}}+u^2\boldsymbol{D}^t\boldsymbol{D})\}^{-1/2} \end{aligned} \tag{73}$$

and the ABIC is given by Eq. (74),

$$\mathrm{ABIC}=-2\ln\int_{-\infty}^{\infty}L(\boldsymbol{x},\sigma^2)p(\boldsymbol{x}\,|\,\sigma^2,u^2)d\boldsymbol{x}$$

$$=2N\ln(2\pi\sigma^2)-K\ln(u^2)+\frac{1}{\sigma^2}\{|\hat{\boldsymbol{A}}\hat{\boldsymbol{x}}-\hat{\boldsymbol{B}}|^2+u^2|\boldsymbol{D}\hat{\boldsymbol{x}}|^2\}+\ln\{\det(\hat{\boldsymbol{A}}^t\hat{\boldsymbol{A}}+u^2\boldsymbol{D}^t\boldsymbol{D})\} \tag{74}$$

The estimate of the variance which minimizes the ABIC is obtained by solving Eq. (75),

$$\frac{\partial(\mathrm{ABIC})}{\partial\sigma^2}=\frac{2N}{\sigma^2}-\frac{1}{\sigma^4}\{|\hat{\boldsymbol{A}}\hat{\boldsymbol{x}}-\hat{\boldsymbol{B}}|^2+u^2|\boldsymbol{D}\hat{\boldsymbol{x}}|^2\}=0 \tag{75}$$

The solution of Eq. (75) is

$$\hat{\sigma}^2=\frac{1}{2N}\{|\hat{\boldsymbol{A}}\hat{\boldsymbol{x}}-\hat{\boldsymbol{B}}|^2+u^2|\boldsymbol{D}\hat{\boldsymbol{x}}|^2\} \tag{76}$$

Finally the ABIC is calculated by the following equation.

$$\mathrm{ABIC}=2N\ln(2\pi)+2N+2N\ln(\hat{\sigma}^2)-K\ln(u^2)+\ln\{\det(\hat{\boldsymbol{A}}^t\hat{\boldsymbol{A}}+u^2\boldsymbol{D}^t\boldsymbol{D})\} \tag{77}$$

Incidentally, the variance given by Eq. (76) is identical to the variance of the residual given by Eq. (69).

In the computation of the ABIC, it is necessary to perform the calculation of the determinant of the matrix in the last term of Eq. (77). A direct calculation of determinant by means of usual methods such as the *Gauss'* sweeping out method often fails to yield the solution, because of the under flow of the digital computation. Hence, the computation herein is performed by utilizing the following relationship (Eq. (78))[16] between the determinant in Eq. (77) and the coefficient matrix obtained in the process of the computation of the estimate $\hat{\boldsymbol{x}}$.

$$\det(\hat{\boldsymbol{A}}^t\hat{\boldsymbol{A}}+u^2\boldsymbol{D}^t\boldsymbol{D})=\prod_{i=1}^{K}S^2_{i,i} \tag{78}$$

where, $S_{i,i}$ denotes the diagonal element of the coefficient matrix (Eq. (66)). Since the direct computation of Eq. (78) also failed in practice, the computation was achieved by handling the logarithm of Eq. (78), *i.e.*

$$\ln\{\det(\hat{\boldsymbol{A}}^t\hat{\boldsymbol{A}}+u^2\boldsymbol{D}^t\boldsymbol{D})\}=\sum_{i=1}^{K}\ln S^2_{i,i} \tag{79}$$

The computation of the estimates of the directional spreading function which is expressed as a piecewise-constant function and the ABIC from the estimates are performed from the given hyperparameter u^2. The hyperparamcter which minimizes the ABIC is found by the method of trial and error. The value of the hyperparameter is given by utilizing Eq. (80) with the value of m changing in a sequential manner.

$$u=ab^m \qquad (m=1,2,\cdots\cdots) \tag{80}$$

The whole procedure mentioned in this section is summarized as follows.

1) For a value of the hyperparameter u given by Eq. (80), compute the estimate of $\hat{\boldsymbol{x}}$ with proper initial value $\boldsymbol{x}_0$.
2) Compute the ABIC by Eq. (77) for the estimate of $\hat{\boldsymbol{x}}$ obtained above.

3) Changing the value of u, repeat the process of 1) and 2).
4) From various estimates of $\tilde{x}$ obtained through the process 1) through 3), choose the values $\hat{u}^2$ and $\hat{\sigma}^2$ as well as the estimate $\hat{x}$ which yields the minimum ABIC as the final estimate of x as the estimate of the directional spreading function.

4. Examination of the estimation method by numerical simulation

4.1 Procedure of numerical simulation

The directional spectrum is expressed as a product of the directional spreading function and the frequency spectrum and is computed frequency by frequency. Hence, in this section, a directional spreading function for an arbitrarily chosen frequency is examined. The practical procedure of the numerical simulation is as follows.

1) The directional spreading functions to be employed in the examination are *Mitsuyasu type* ones[20),21)] which are given by Eq. (81).

$$G(\theta)=\sum_i \alpha_i \cos^{2S_i}\left(\frac{\theta-\theta_i}{2}\right) \tag{81}$$

where α_i is the proportionality coefficient and is given so that Eq. (81) satisfies Eq. (5). For the simulation of a uni-directional sea, the directional spreading function is given by Eq. (81) with $i=1$ only. On the other hand, for a bi-directional sea, two different wave groups having different values of α_i, S_i, θ_i $(i=1, 2)$ are superimposed.

2) The cross-power spectra are computed for the directional spreading function given by process 1) utilizing Eq. (3). When the estimation errors of the cross-power spectra are taken into account, normal random values having the mean 0 and the standard deviation σ_R (for the real part of the cross-power spectra) or σ_I (for the imaginary part of the cross-power spectra) added to the cross-power spectra calculated above. The values of the standard deviation σ_R and σ_I are given by multiplying the absolute value of the real the imaginary part of the cross-power spectrum by some factors (0.0025, 0.01, ..., 0.16).
3) On the basis of the cross-power spectra obtained above, the directional spreading function is estimated by means of the methods mentioned in the previous section. The estimate of the directional spreading function is compared with the input directional spreading function, *i.e.* the one given by Eq. (81). In addition, the directional spreading functions are also estimated by the EMLM for the comparison of those given by the Bayesian approach.

The process of the analysis of the directional spectrum consists of two steps. The first step is to estimate the cross-power spectra for the given time series records of wave properties. The second step is to compute the estimate of the directional spreading function from these estimated cross-power spectra. Thus, there are two possible stages where errors occur. This section discusses how the errors in the second stage differ for different estimation methods. This is done for the convenience of comparison between the input and the output directional spreading function, and the numerical simulation in this section is performed for the second step and the cross-power spectra are calculated direct numerical integration of Eq. (1), and therefore the cross-power spectra to be utilized herein as the input data do not contain any errors unless they are intentionally added.

4.2 Conditions employed in the simulation and the directional spectrum

Seven types of the arrays of wave probes shown in Fig. 2 are examined. The wave conditions η, η_x and η_y in the figure denote the wave probes which detect water surface elevation, the slope of the water surface in the direction x and the water surface slope in the direction y, respectively.

The parameter S in Table 2 is the power of the directional function (see Eq. (81)), and $S=10$ represents the wind generated waves, while $S=100$ represents long traveled swell. The parameter $\Delta\theta$ denotes the angle between the mean wave directions of the two different wave groups.

In the computation of the estimates of the directional spreading function by the Bayesian approach, the initial values of $\boldsymbol{x}_0$ (logarithm of the directional spreading function) are given uniformly ($x_i=\ln(1/2\pi)$). The iteration of Eq. (59) in the estimation of the directional spreading function is terminated when the standard deviation of the difference between the values of $\boldsymbol{x}_n$ of n-th step and that of the previous step is smaller than or equal to 10^{-3}, *i.e.*

$$|\sigma_{\varepsilon n}| \leqq 10^{-3} \tag{82}$$

Finally, the values $\boldsymbol{x}_n$ obtained in n-th step are considered as the estimate of $\boldsymbol{x}$.

When the iteration does not converge within the condition Eq. (82), the following treatment were done.

1) When the standard deviation of the difference between $\boldsymbol{x}_{n-1}$ and $\boldsymbol{x}_n$ once shows its minimum value and then fluctuates, the iteration is continued for a few more

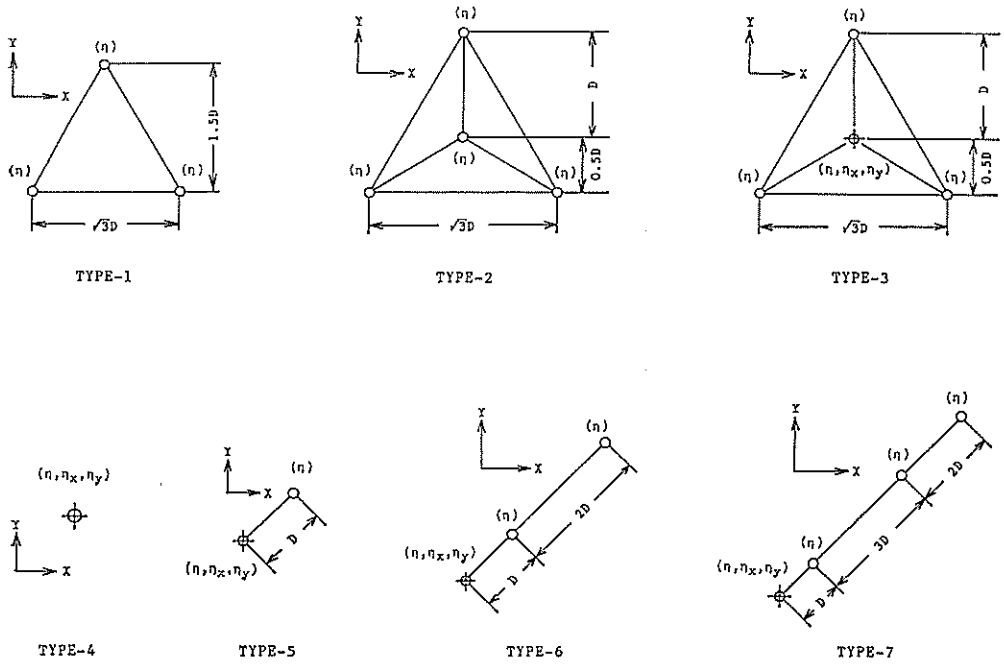

Fig. 2 Types of wave probe array examined by numerial simulation

steps. The values of x_n which give minimum $\sigma_{\varepsilon n}$ among the whole steps are considered as the estimates.

2) When the standard deviation $\sigma_{\varepsilon n+1}$ for $(n+1)$th step iteration is ten times greater than that of the n-th step $\sigma_{\varepsilon n}$, the iteration is terminated immediately and the set of values of x which yield a minimum among the previous steps are chosen as the estimates.

3) When the iteration does not make a standard deviation smaller than the conversion condition even after 100 steps, the computation is terminated, and the values x_n which give the smallest $\sigma_{\varepsilon n}$ are printed out for reference.

The values of the hyperparameter u are given by Eq. (80), and the coefficients a, b, and m in Eq. (80) are given the following values on the bases of a trial computation.

$$a=0.2,\ b=0.5,\ m=1,\cdots\cdots,20. \tag{83}$$

(for the cases that no errors are added to cross-power spectra)

$$a=51.2,\ b=0.5,\ m=1,\cdots\cdots,20. \tag{84}$$

(for the cases that errors are added to the cross-power spectra)

Though the value of m is changed from 1 to 20, as shown in the above equations, the computation is terminated at any value of u if the ABIC shows minimum value and then increases for succeeding values of m.

4.3 Examination of the estimation methods

(1) Effect of types of probe array

The results of the simulations are shown in Fig. 3 for the 7 types of arrays of wave probes (see Fig. 2). The same wave condition is employed for all the arrays: wind waves characterized by $S=10$ coming in the direction $\theta_1=0°$ and a swell characterized by $S=100$ coming in the direction $\theta_2=100°$ coexist, and the ratio of the peak spectral density of the two wave groups is $a_1/a_2=0.5$.

In addition, the distance between the wave probes D is given as $D/L=0.2$ (L is the wave length of the component wave to be examined) for all the arrays. The solid lines denoted by TRUE in Fig. 3 show the input directional spreading function, and the lines noted by BDM shows the estimate of the directional spreading function given by the Bayesian directional spectrum estimation method (which is called BDM hereafter). The ordinate of Fig. 3 is normalized utilizing the peak value of the input directional spreading function for respective cases as reference value.

Comparing the estimates of the directional spreading functions result from Type-1 through Type-3 in Fig. 3, as the number of wave probes increases, the directional resolution shown by the BDM and the EMLM is improved. In paticular, the estimates given by BDM for Type-2 and Type-3 are almost the same as the input directional spreading function. The estimates given by the EMLM are improved for Type-3 in comparison with those for Type-2 and Type-1. Though, for Type-1 layout, the estimate given by the EMLM seems to be closer to the true directional spreading function than that given by BDM, for Type-2 layout, the EMLM yields an erroneous peak inbetween the two peaks exhibited by the true directional spreading function. The estimate given by EMLM is considerably improved for Type-3 in comparison with the estimate for Type-2, but the resolution is inferior to that of the BDM.

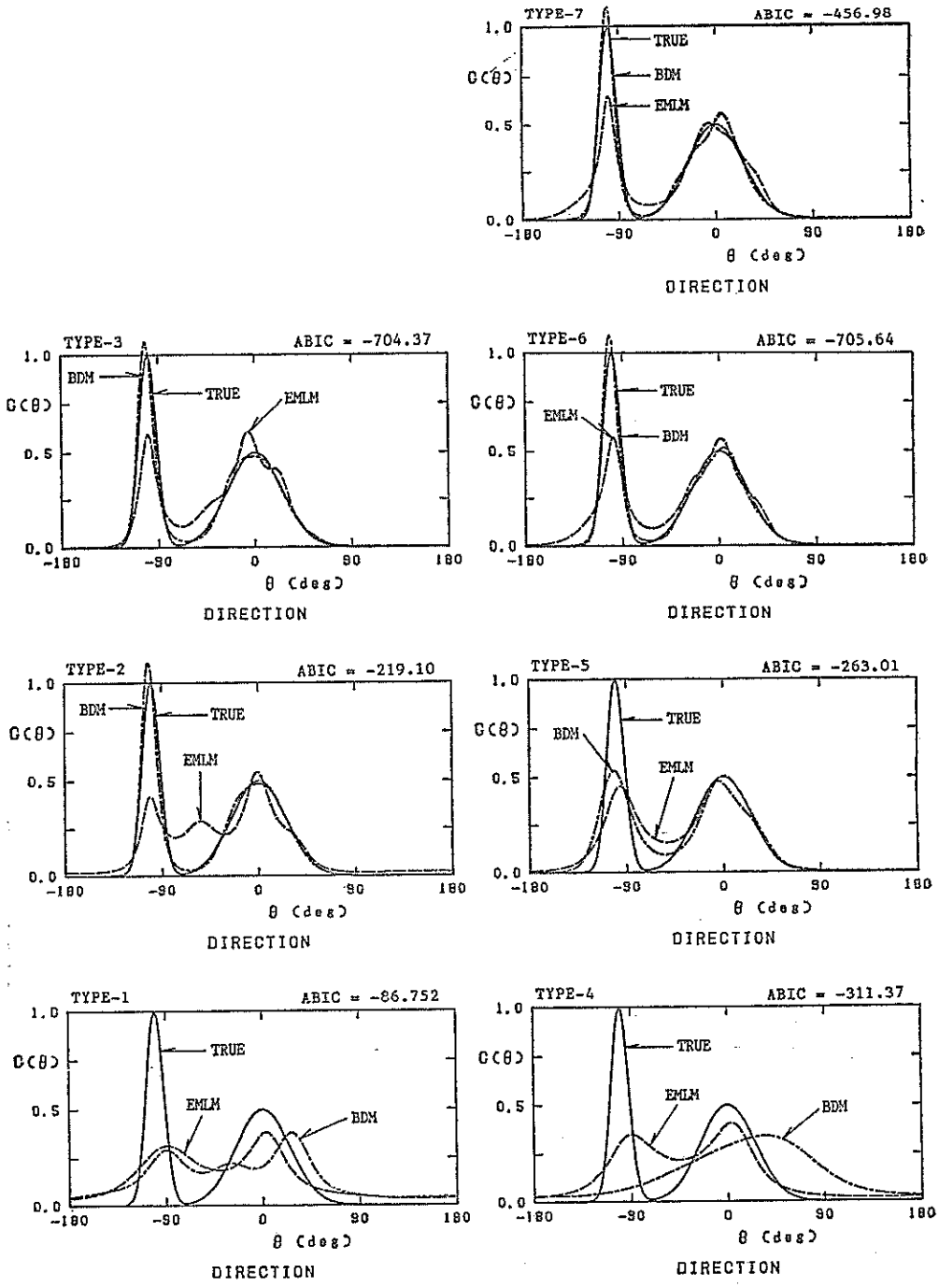

Fig. 3 Directional spreading functions estimated from various types of probe arrays

For the wave prove arrays consisting more than or equal to 4 probes, it is seen that the BDM shows a better directional resolution than that of the EMLM.

From the comparison of the results for Type-4 through Type-7 in Fig. 3, it is said that as the more wave probes are employed, the higher directional resolution is exhibited by both of the BDM and the EMLM. Obviously, the BDM shows the better resolution than the EMLM for Type-5 through Type-7. Especially for Type-6 and Type-7, only minor discrepancy is observed between the estimated and the input directional spreading function. However it should be noted that, for Type-4, the BDM yields an estimate quite different from the input directional spreading function.

For Type-1 and Type-4, only three wave probes are utilized to measure the directional seas. The BDM does not find a suitable statistical model to explain bi-directional sea. In other words, as stated in section 2, three independent wave properties are the minimum data to analyze the directional spectrum, and so it is impossible to estimate the errors contained in the estimation of the cross-power spectra from three-element measurement. Hence the reason why the BDM fails to give a proper estimate is supposed to be the fact that the method cannot distinguish between two different wave groups due to the introduction of the errors ε_i.

On the other hand, the Maximum Entropy Principle Method (MEP) does not consider the errors associated with the cross-power spectra, and the models handled by the method are not statistical ones but parametric ones. Therefore, the MEP successfully distinguishes two different wave groups for the cases $\Delta\theta > 90°$[9].

From the comparison between the results of the estimation shown in Fig. 3, it

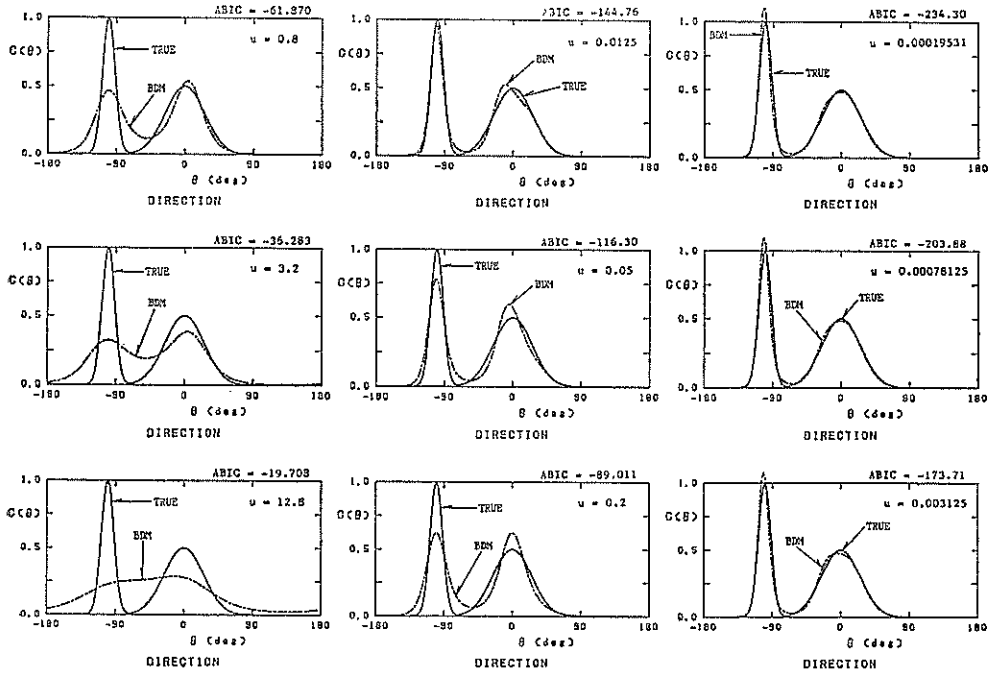

Fig. 4 Estimates of directional spreading functions and the values of ABIC for different values of the hyperparameter u (Type-2 Star array)

can be said that the BDM shows a better resolution than other methods when wave records consisting four or more elements are available, though the method has a shortcoming when the wave records consisting of three elements only are available.

The comparison between the results for Type-2 and that for Type-5 implies that the precision of the estimation varies depending on the types of the wave probe array. Even though the BDM is less sensitive to the layout of the sensor array than the EMLM and the Direct Fourier Transformation Method, careful examination of the layout of the sensor array is recommended before the wave observation is conducted.

(2) Relation between the hyperparameter and the directional resolution

For the wave probe array of Type-2 having the distance between probes $D/L=0.2$, the relationship between the hyperparameter u, and the directional resolution of the estimates and the values of the ABIC (see Eq. (87)) are examined. Figure 4 shows how the estimated directional spreading function varies as the hyperparameter u decreases from 12.8 to 0.00019531. The hyperparameter is a sort of weighting coefficient for the smoothness of the directional spreading function against the restriction condition which is the mathematical relationship between the cross-power spectra and the directional spectrum. Thus, for a large value of the hyperparameter u, the resulting estimate shows quite a mild shape. As the value of the hyperparameter decreases, the directional spreading function becomes sharper, and the value of the ABIC associated with the resulting estimates decreases, which implies that the estimate is more suitable. In fact, the estimate became closer to the true directional spreading function as the ABIC decreases.

For the cases where u is less than 0.00019531, the iteration does not converge within the condition Eq. (82), and the estimate obtained for minimum ABIC (ABIC$=-234.30$, $u=0.00019531$) is chosen as the final estimate for the sea state. It is seen the BDM yields quite a reasonable estimate.

(3) Estimation for various sea states

(a) uni-directional sea

Figure 5 shows the estimates given by the BDM for uni-directional seas having various directional spreading characteristics. The estimates given by the EMLM for the seas where the wave energy is wide-spread show an ill-conditioned shape, while those given by the BDM are quite smooth even for the extreme case $S=1$ where the wave energy is spread over a wide range of direction.

(b) Bi-directional seas

Figures 6 to 10 show the results for various bi-directional seas. For all these figures, the wave probe array employed is Type-2 shown in Fig. 2. Figure 6 shows sea states consisting of wind generated waves having $S=10$ and a swell having $S=100$ and the same peak spectral density as the wind generated waves. Figure 7 shows the results for sea states where there are wind generated waves, and a swell for which the peak spectral density is a half of that of the wind generated wave coexist. Figure 8 is drawn for sea states where the peak spectral density of swells is twice as much as that of the wind generated waves. On the other hand, Fig. 9 shows the results for sea states where two different swells having the same magnitude of the peak spectral density coexist, while Fig. 10 shows the results for the cases the magnitude of one swell is half of the other.

The computation is done for various magnitudes of the differences between the mean wave direction of the two wave groups. These figures show that the estimate

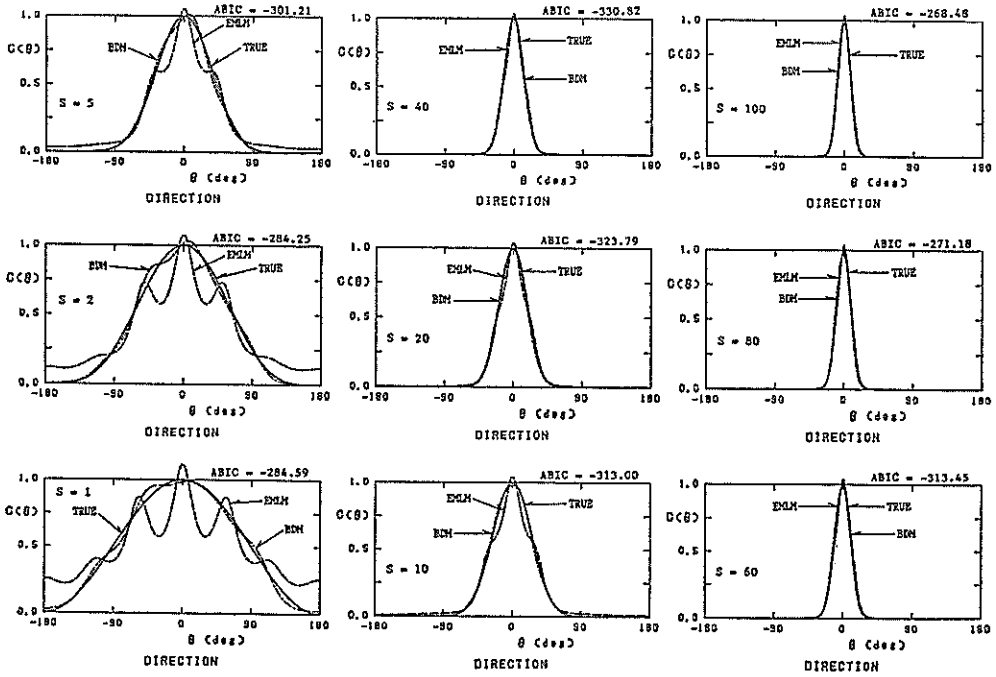

Fig. 5 Estimates of directional spreading functions for uni-directional sea (Type-2 Star array, Case-1～Case-9 in Table 2)

Table 2 Wave conditions employed in the numerical simulation

Case-1～9	Case-10～18	Case-19～27	Case-28～36	Case-37～45	Case-46～54
uni-directional	bi-directional sea				
	$S_1=10$ $S_2=100$ $\alpha_1/\alpha_2=1.0$	$S_1=10$ $S_2=100$ $\alpha_1/\alpha_2=2.0$	$S_1=10$ $S_2=100$ $\alpha_1/\alpha_2=0.5$	$S_1=100$ $S_2=100$ $\alpha_1/\alpha_2=1.0$	$S_1=100$ $S_2=100$ $\alpha_1/\alpha_2=2.0$
$S=1$	$\Delta\theta=20°$				
$S=2$	$\Delta\theta=40°$				
$S=5$	$\Delta\theta=60°$				
$S=10$	$\Delta\theta=80°$				
$S=20$	$\Delta\theta=100°$				
$S=40$	$\Delta\theta=120°$				
$S=60$	$\Delta\theta=140°$				
$S=80$	$\Delta\theta=160°$				
$S=100$	$\Delta\theta=180°$				

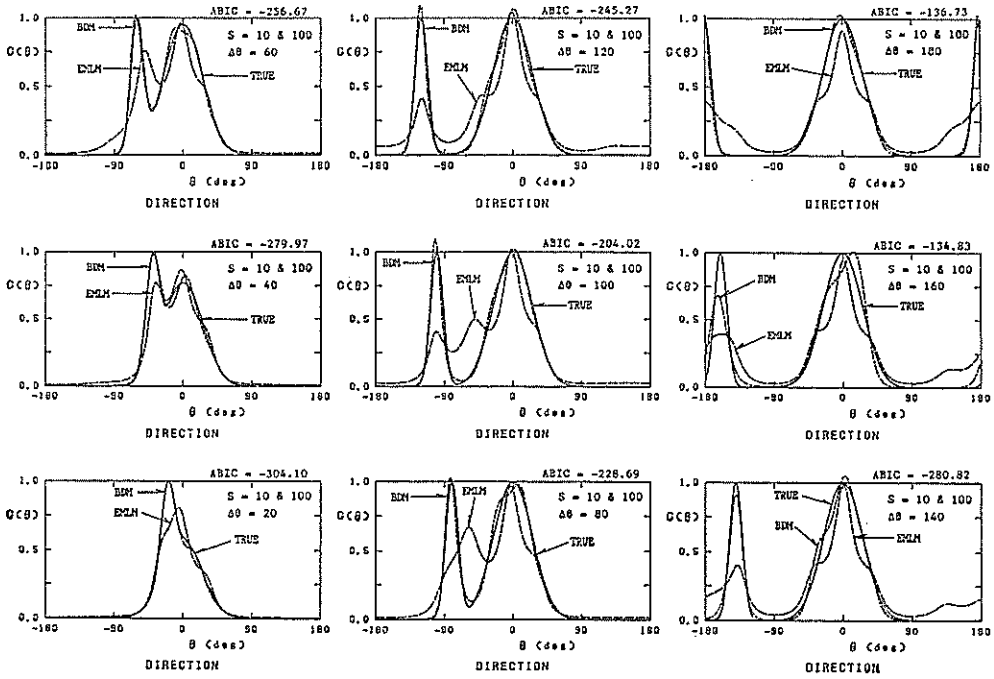

Fig. 6 Estimates of directional spreading functions for bi-directional sea (Type-2 Star array, Case 10~Case-18 in Table 2)

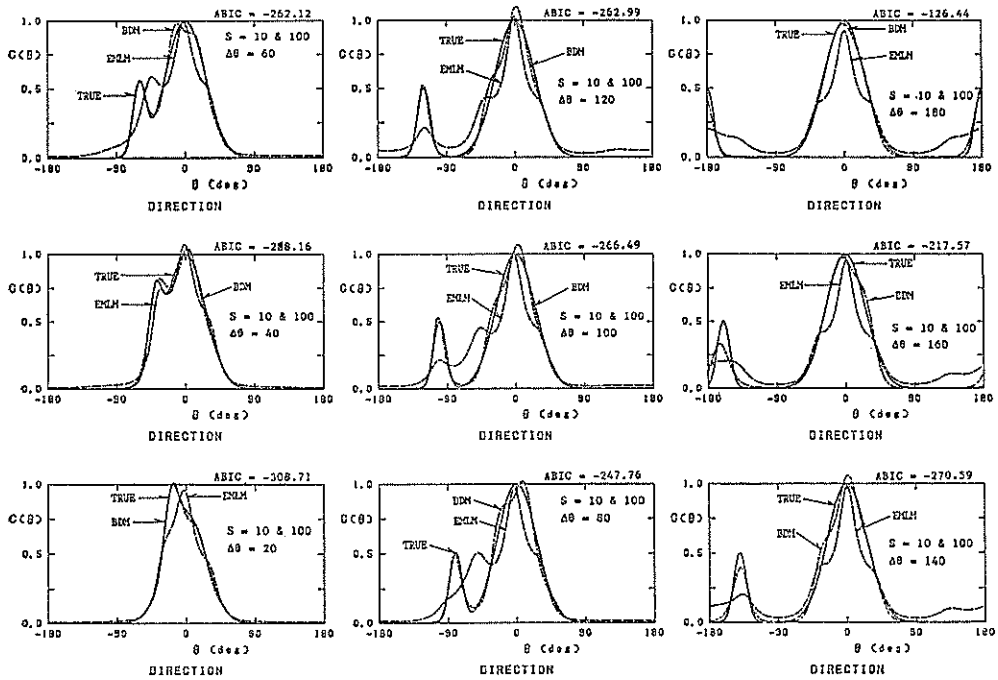

Fig. 7 Estimates of directional spreading functions for bi-directional sea (Type-2 Star array, Case 19~Case 27 in Table 2)

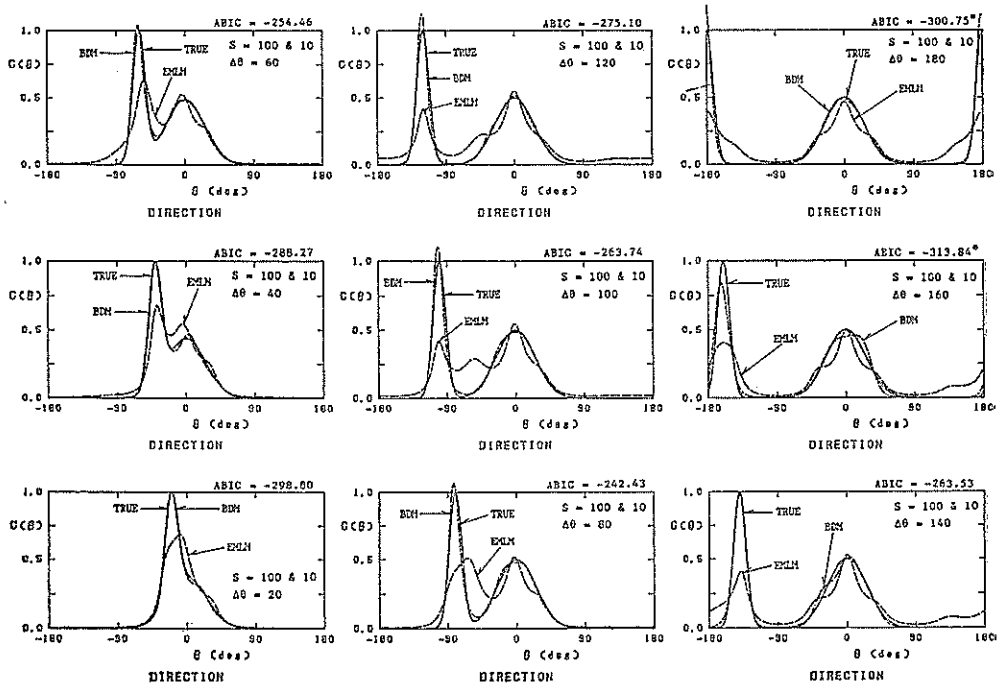

Fig. 8 Estimates of directional spreading functions for bi-directional sea (Type-2 Star array, Case-28～Case-36 in Table 2)

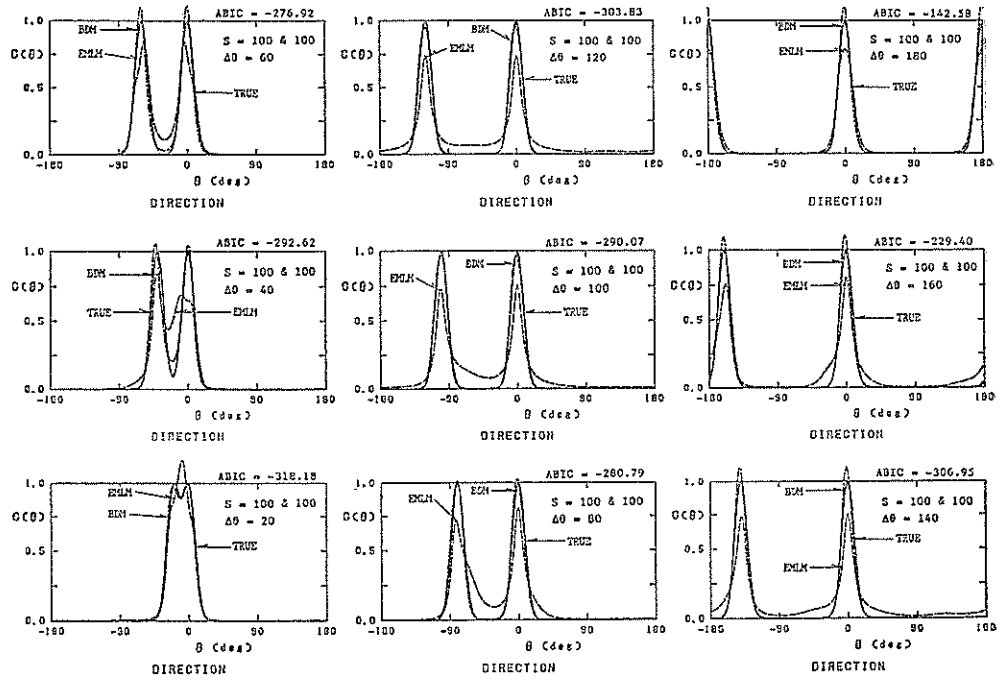

Fig. 9 Estimates of directional spreading functions for bi-directional sea (Type-2 Star array, Case-37～Case-45 in Table 2)

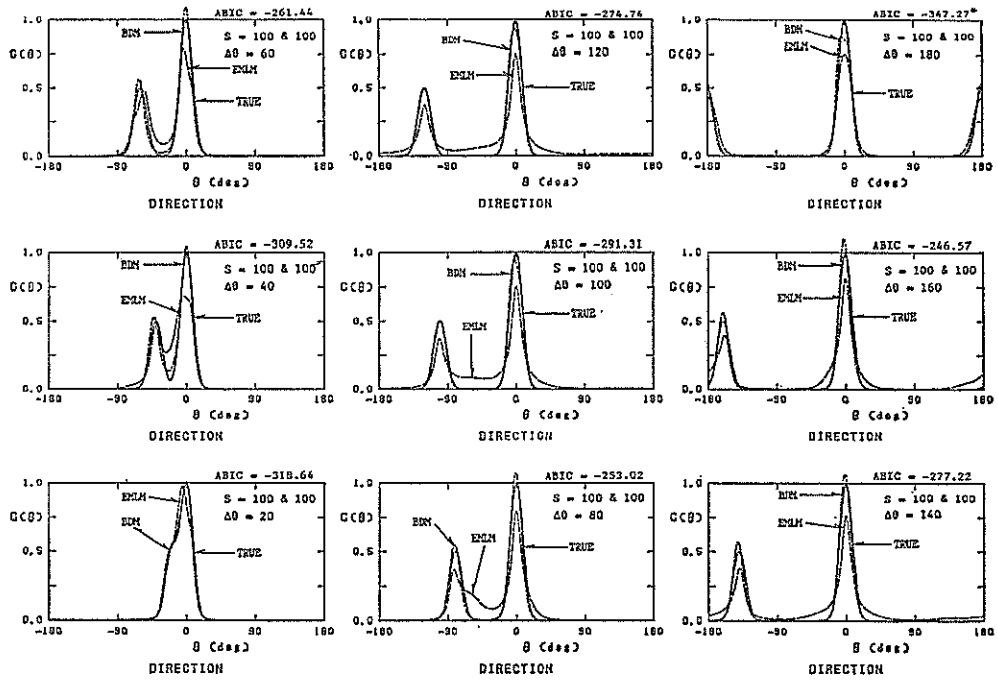

Fig. 10 Estimates of directional spreading functions for bi-directional sea (Type-2 Star array, Case 46~Case 54 in Table 2)

of the directional spreading function yielded by the BDM are very close to the true ones. On the other hand, those obtained by the EMLM show smaller peak values for all the cases than those of the true ones, while some leakage of the wave energy is observed where the true directional spreading functions are zero. In addition, the EMLM cannot detect two different peaks when the difference of the directions of the two wave group is small ($\Delta\theta$=20°), while this difference is obvious for the BDM.

Hence, it can be expected that when the wave probe array of Type-2 is employed, the estimates given by the BDM are very accurate for any kinds of bi-directional seas.

Incidentally, the upper right figure of Fig. 10 marked with * is the case that the iteration computation (Eq. (59)) does not converge within the condition Eq. (82), and the results when computation is terminated are plotted for reference, but the estimate is quite close to the true directional spreading function.

(4) Effect of errors contained in the cross-power spectral estimates

The effect of the errors contained in the cross-power spectra is examined in Fig. 11. The prove array employed is Type-2. The estimates for different magnitudes of the errors are shown in the figure. The ratio of the error added to the cross-power spectra is denoted by r in the figure, and the value of r is changed from 0.0 to $(0.4)^2$ with the interval of $(0.05)^2$.

The values of r in the figure show the magnitudes of the error contained in the cross-power spectra, which are expressed as the ratio of the error and the root

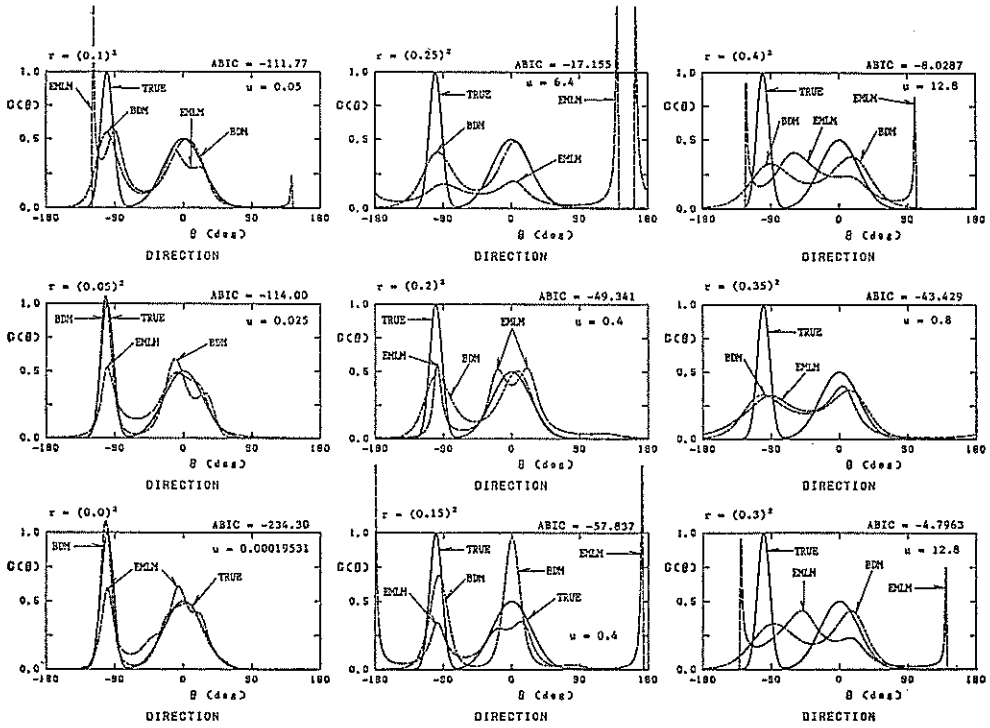

Fig. 11 Effect of noise in cross-power spectra on the estimates of directional spreading functions (Type-2 Star array)

mean square of the absolute values of the real part and the imaginary part of each cross-power spectrum. The magnitude of the errors is expressed in a quadratic form, because the cross-power spectra are proportional to the amplitudes of the time series variation of wave properties. By the use of this expression, the rate of the error over the magnitude of the true variation of wave properties is easily understood. In the computation, the same magnitude of the error is multiplied to all the four wave properties, for each case.

It is noted that as the magnitude of errors increases, the information about the directional spectrum carried by the cross-power spectra becomes more biased one. In fact, as seen in Fig. 11, the estimates given by the BDM became flatter as the magnitude of error increases. It is also seen that the BDM yields quite accurate estimates even if the time series records contain 5% errors. When the cross-power spectra contain larger errors, the EMLM estimates erroneous peaks and sometimes fails to yield smooth and continuous estimates of the directional spreading function. On the other hand, the BDM detects the direction of the peaks properly, although it underestimates the peak values. Thus, the BDM seems to be very sound and stable against errors.

(5) Effect of the dimension of probe array

For Type-2 wave probe array, the directional spreading functions are estimated for various dimensions of the array. Figure 12 shows how the estimates vary depending on the ratio of minimum distance of the wave probes and the wave length

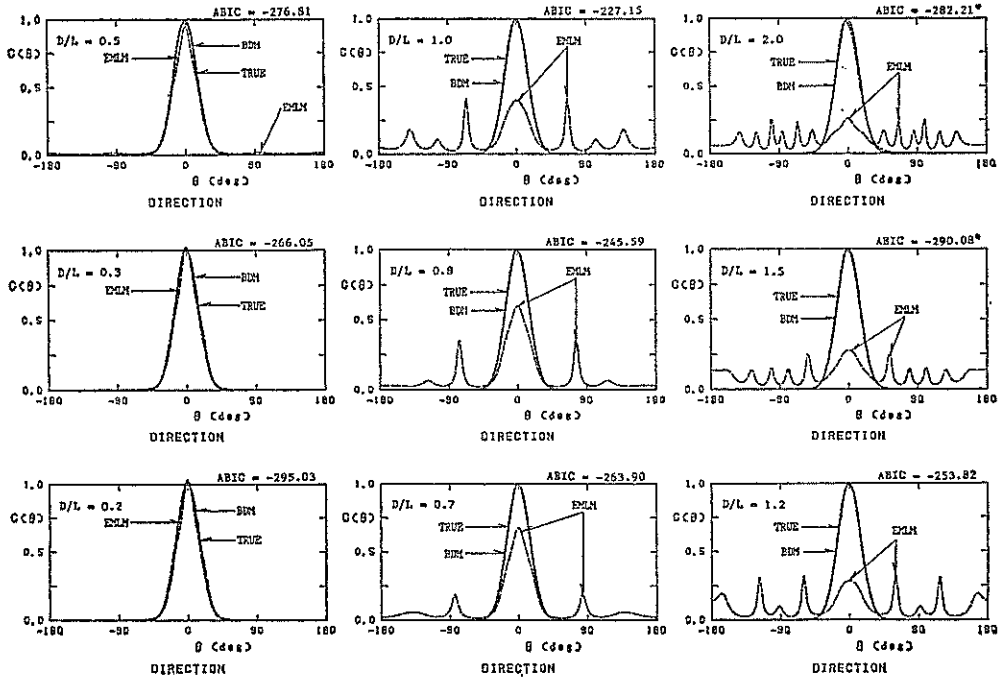

Fig. 12 Effect of the dimension of the probe array (Type-2 Star array)

L. The wave condition employed is a uni-directional sea characterized by S=30. It is obviously seen that the estimates given by the EMLM show an erroneous side lobe when D/L is larger than 0.5. On the other hand, the estimates given by the BDM are fairly close to the true directional spreading function even the ratio D/L is 2.0, though the iteration did not converge within the condition Eq. (82) for the cases D/L=1.5 and 2.0, which are marked with * in Fig. 12.

Estimates having side lobes which are given by the EMLM are also considered as one of the solutions which satisfies the relationship expressed by Eq. (3), while the BDM chooses the simplest one on the basis of the balance between the likelihood and the smoothness of the directional function.

As *Goda*[3] recommended the wave probe array should be arranged so that the minimum distance between the probes is less than 0.5 times the smallest wave length among the waves to be measured. However, when the BDM is employed for the analysis, this restriction can be eased. This is very advantageous, because the real ocean waves consist of many component waves having various frequencies and a small dimension of the wave probe array results in lower directional resolution for longer and shorter period waves.

(6) Effect of the number of segments of directional spreading function

In the computation stated above, the estimate of the directional spreading function is given by piecewise constant function which consists of 180 segments. The computation takes time in the matrix calculation of Eq. (59). Therefore, how the results are affected by the number of the partitions of the directional spreading function is examined. Figure 13 shows the estimates for various numbers of parti-

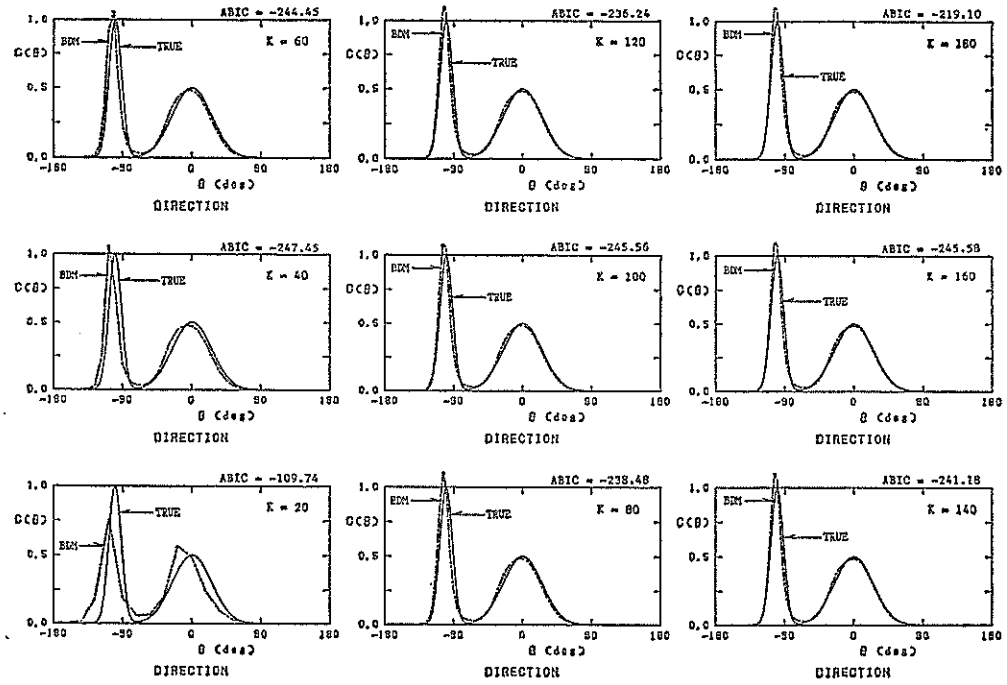

Fig. 13 Effect of the number of partitions of directional spreading function (Type-2 Star array)

tions of the function. It is seen that when the number of partition is small, say $K=$ 40, the estimated directional spreading functions are very close to the true ones.

5. Field data analysis

5.1 Facilities of directional wave measurement

The new method for the estimation of the directional spectrum on the bases of the Bayesian approach mentioned above is applied to the analysis of the wave records acquired at an offshore oil rig 42 km off the *Iwaki* coast (Northeastern coast of the main island of Japan, see Fig. 14). The *Onahama* Port Construction Office (OPCO), the Second Port Construction Bureau, Ministry of Transport, is conducting a multi-element measurement of ocean waves at this location. Figure 15 shows the oil rig where four step type wave gauges and a two-axis directional current meter with a pressure sensor are installed on its legs as shown in Fig. 16. The location of the rig is 37°17′49″N and 141°27′47″E, in a water depth of 155 m below C.D.L.

The simultaneous measurement of 7 elements is performed for 20 minutes at a time interval of two hours. The wave records as well as the wind records are immediately transmitted by a radio telemetering system to a nearby coastal relay station for landline transmission to the OPCO.

The time series wave data are recorded on a digital magnetic tape. Data are also analyzed immediately following each observation using a mini-computer of the

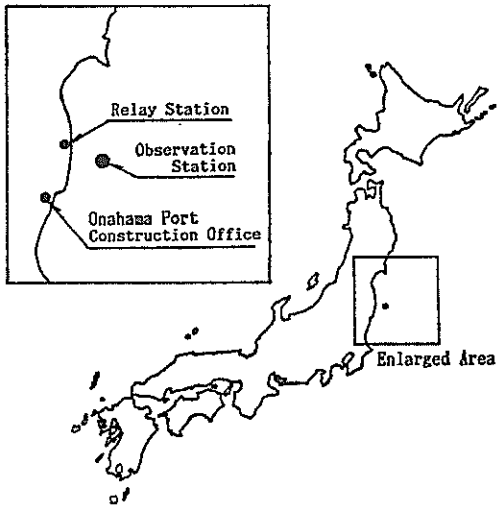

Fig. 14 Location of the observation station

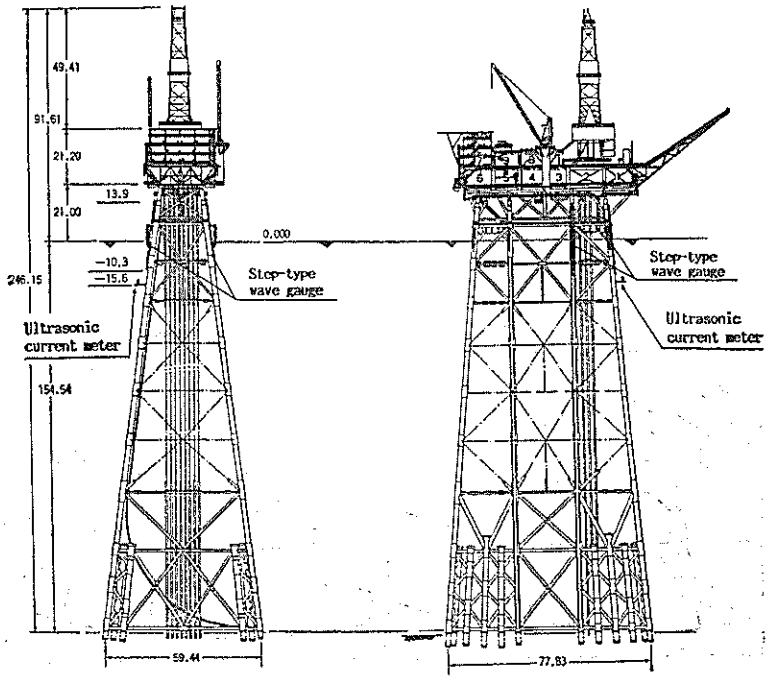

Fig. 15 Offshore oil rig and the location of wave probes

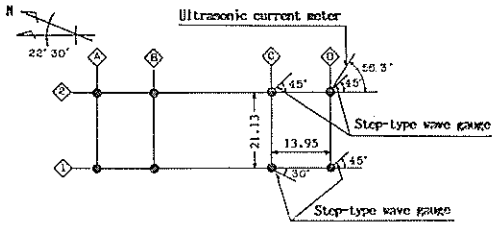

Fig. 16 Wave probe array

OPCO for real time information such as significant wave height, wave period and mean wave direction. The EMLM is employed for the real time directional analysis at the office. The directional wave analysis presented herein is performed at the Port and Harbour Research Institute using the wave data recorded on the magnetic tapes.

5.2 Estimates of directional spectrum

(1) Wave data to be analyzed

The time series wave records analyzed here were obtained during the passage of Typhoon No. 17 from September 29 to 30 in 1986. The typhoon passed by the rig from the south to the northeast. At 12:00 on September 30, the maximum significant wave height ($H_{1/3}$=6.20 m) and period ($T_{1/3}$=12.5 s) was recorded at the rig. Figure 17 is the weather maps of these two days. Typhoon No. 17 was one of the strongest to hit Japan in 1986.

The cross-power spectra which are utilized in the estimation of the directional spectrum are computed by Eq. (85).

$$\Phi_{ij}(f)=C_{ij}(f)-iQ_{ij}(f)=\int_{-\infty}^{\infty}\Psi_{ij}(\tau)\exp(-i2\pi f\tau)d\tau \tag{85}$$

where C_{ij} and Q_{ij} are the co-spectrum and the quadrature-spectrum respectively, and $\Psi_{ij}(\tau)$ is the covariance function between the two properties ξ_i and ξ_j. The covariance function are computed by Eq. (86).

$$\Psi_{ij}(\tau)=\overline{\xi_i(t)\xi_j(t+\tau)} \tag{86}$$

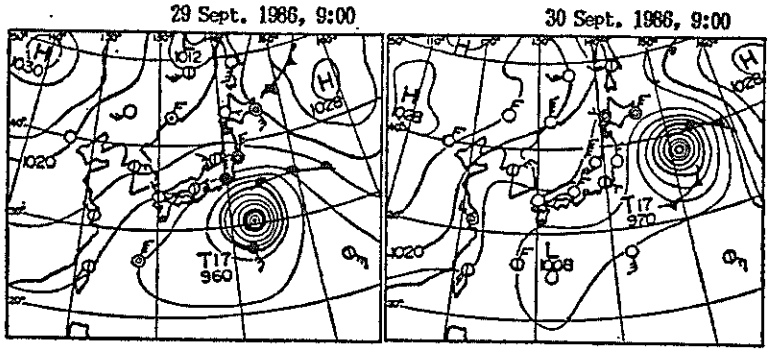

Fig. 17 Weather maps of Typhoon No. 17 (29-30 Sept. 1986)

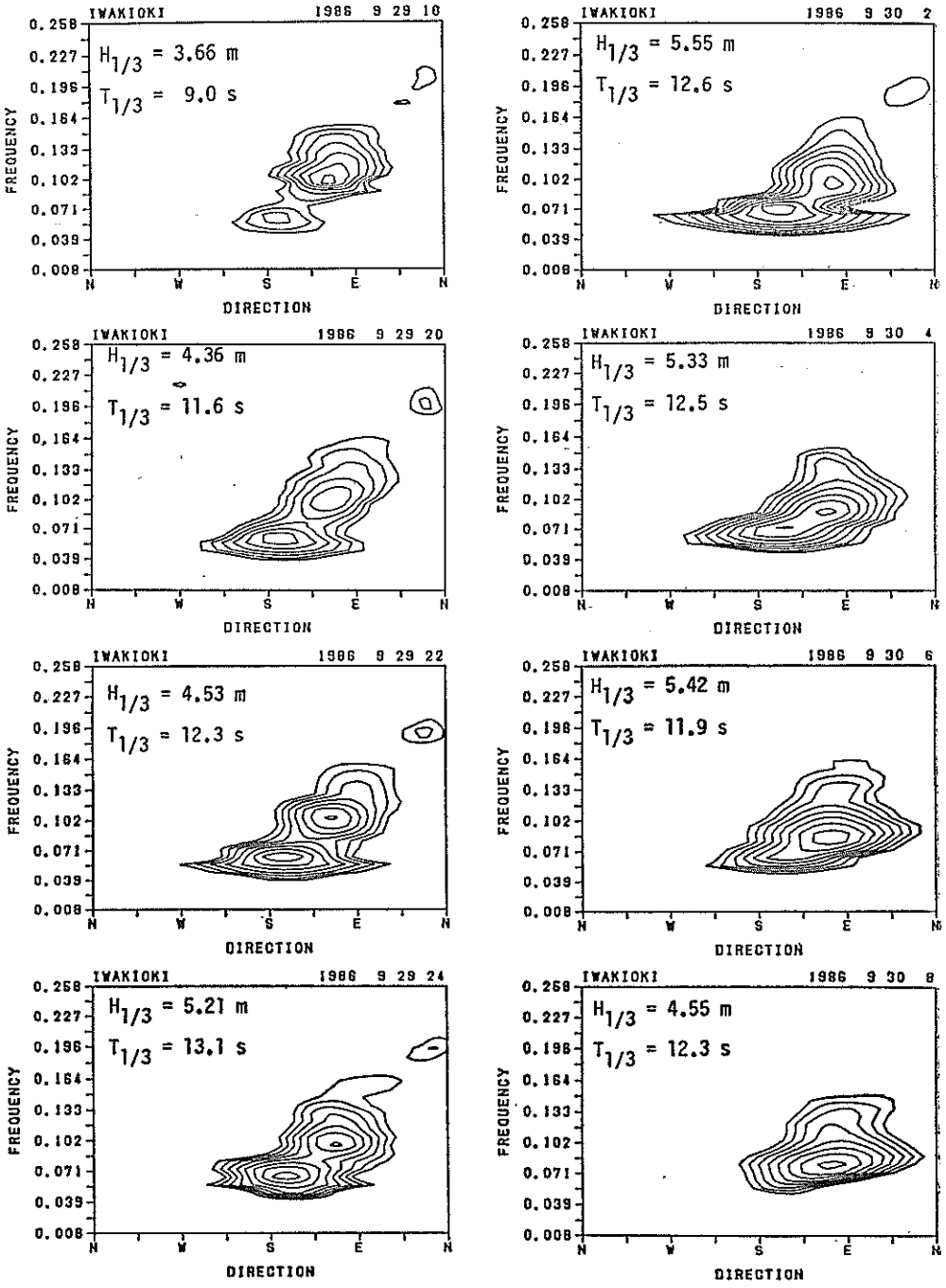

Fig. 18 Time variation of the directional spectrum (estimated by the BDM from 7-element measurement)

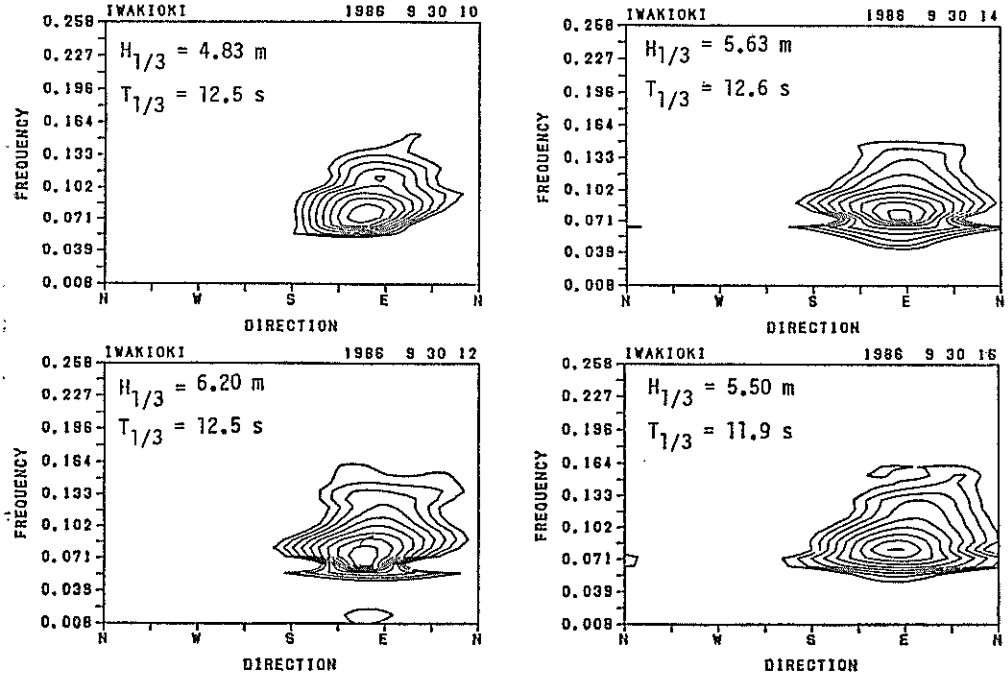

Fig. 18 Time variation of the directional spectrum (continuation) (estimated by the BDM from 7-element measurement)

(2) Estimates of the directional spectra

Figure 18 shows the time variation of the directional spectrum estimated on the basis of the 7-element wave records by the BDM for every two hours from 18:00 on Sept. 29 to 16:00 on Sept. 30. Up to 4:00 on Sept. 30, bi-directional seas are observed: swells come from the south and the wind generated waves come from the east-southeast at the same time. After 6:00 on the 30th, the directional spectra are uni-directional. During the passage of Typhoon No. 17, the significant wave height shows two maxima. One was observed at 2:00 on the 30th, when the spectral density of the swell reaches its maximum. The other peak significant wave height was observed at 12:00 on the 30th and it was the highest during these two days. It should be noted that the directional spreading function of the directional spectra observed at 12:00 and later are constricted at the peak frequency, *i.e.*, the concentration of the spectral density is the highest at the peak frequency and becomes lower as the frequency deviates from the peak frequency. This is the same characteristics shown in the directional spreading function proposed by *Mitsuyasu*[20].

Examples of the directional spectra estimated by the BDM and EMLM for uni-directional seas are compared in Fig. 19. The upper figures are the schematic showing of the spectra and lower figures are the plane showing of respective spectra with contour lines. The major difference between the two estimation methods is that the EMLM is more diffuse and does not show a constriction near the peak frequency clearly depicted in the BDM estimated by the BDM. It is also clear that the peak spectral density given by the EMLM is much lower than that given by

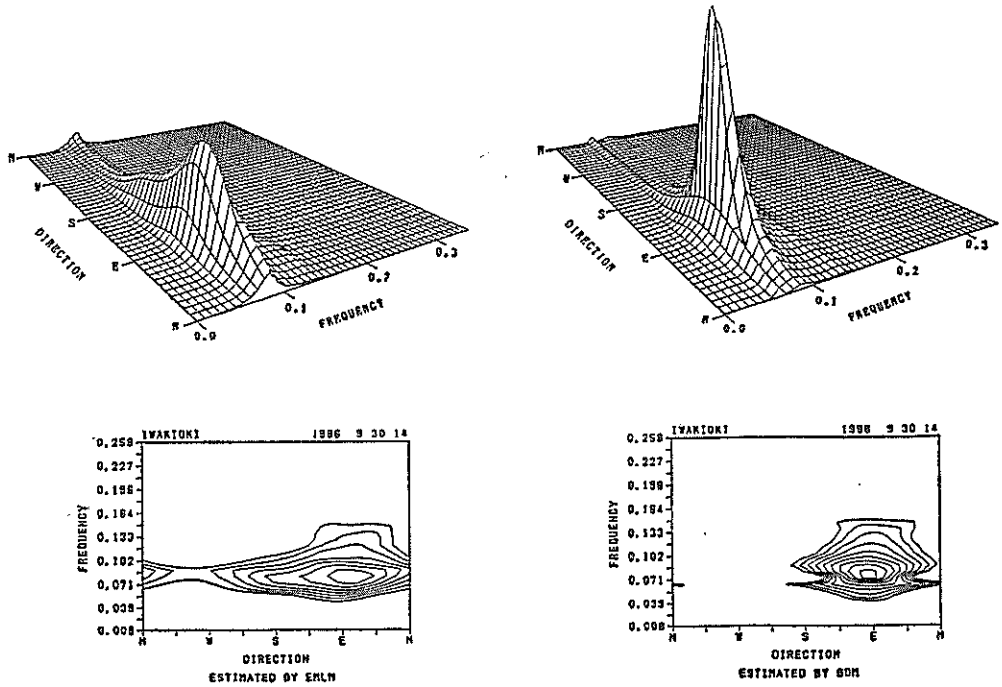

Fig. 19 Uni-directional spectrum observed at 14: 00, 30 Sept. 1986 (7-element measurement)

the BDM.

For the same sea as shown by Fig. 19, the directional spectrum is estimated from three-element wave record only, *i.e.* the wave record obtained by the two-axis directional current meter and the pressure sensor. Figure 20 shows the comparison of the directional spectra estimated by the EMLM and the MEP. Neither of the two methods can detect the constriction shown by the estimate given by the BDM for the 7-element measurement (see Fig. 19). The estimate given by the MEP shows higher peak spectral density than that given by the EMLM, and the peak spectral density given by the MEP is almost the same as that given by the BDM for the 7-element measurement.

Figure 21 is drawn in the same way to show examples of the estimates on the basis of the 7-element measurement for a bi-directional sea observed at 22:00 on Sept. 29. It is seen in Fig. 21 that, again, the estimate given by the BDM shows higher spectral peaks than those shown by the estimates given by the EMLM, especially the spectral peaks of the wind generated waves.

Figure 22 shows the bi-directional spectra estimated from the three-element measurement. Compared with Fig. 21, it is seen that EMLM yields almost the same shape of the spectral estimate for the 7-element measurement. Figure 22 also shows that the MEP yields more concentrated estimate with higher peak density for the swell than the estimate by the BDM shown in Fig. 21.

On the basis of these results, we conclude that the estimates of the directional spectra show different shapes depending on the method for the estimation and the number of the elements of the wave properties utilized. In addition, though a three-

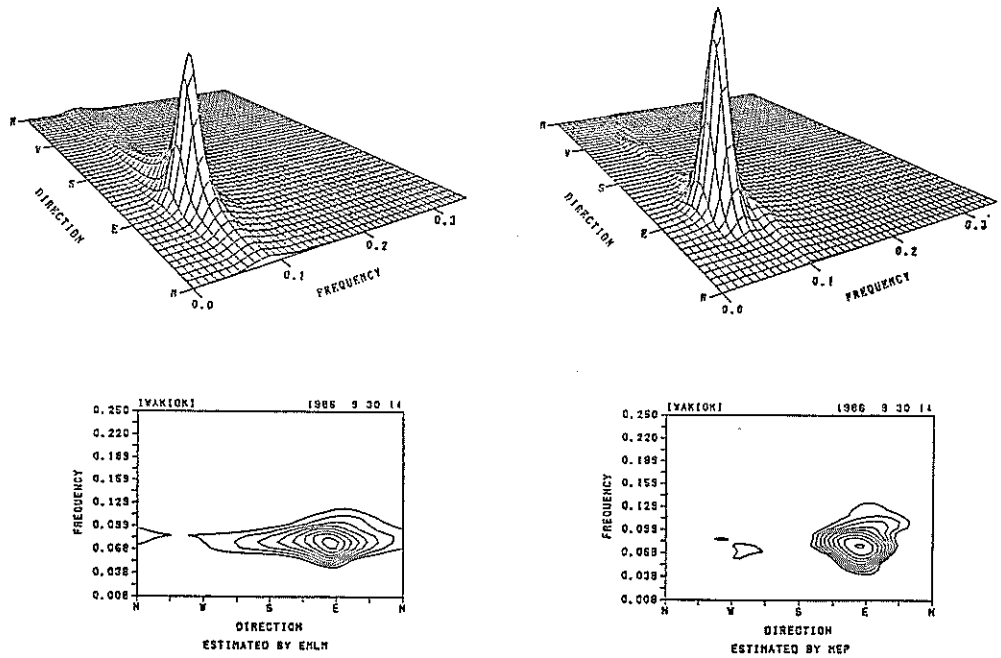

Fig. 20 Uni-directional spectrum observed at 14: 00, 30 Sept. 1986 (3-element measurement)

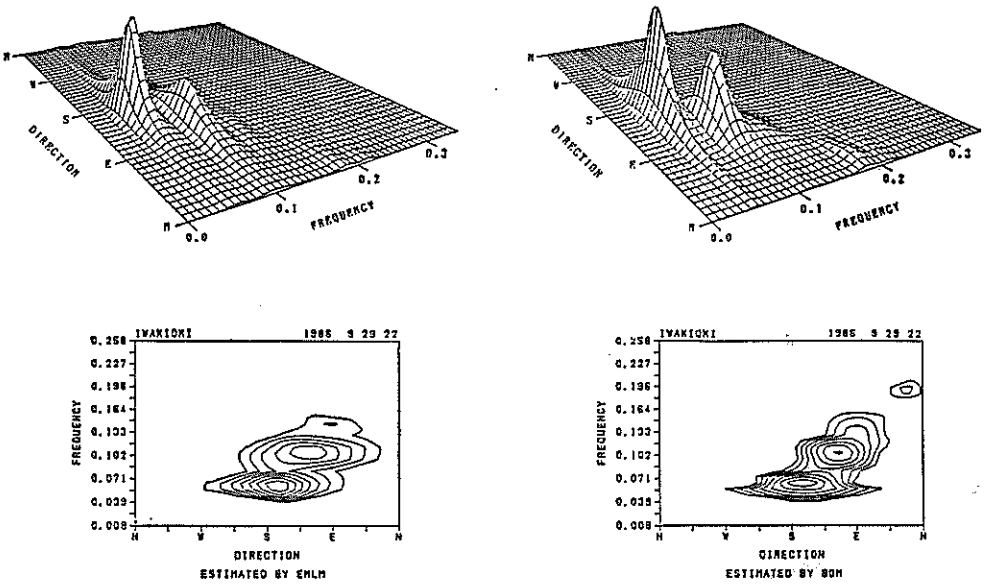

Fig. 21 Bi-directional spectrum observed at 22: 00, 29 Sept. 1986 (7-element measurement)

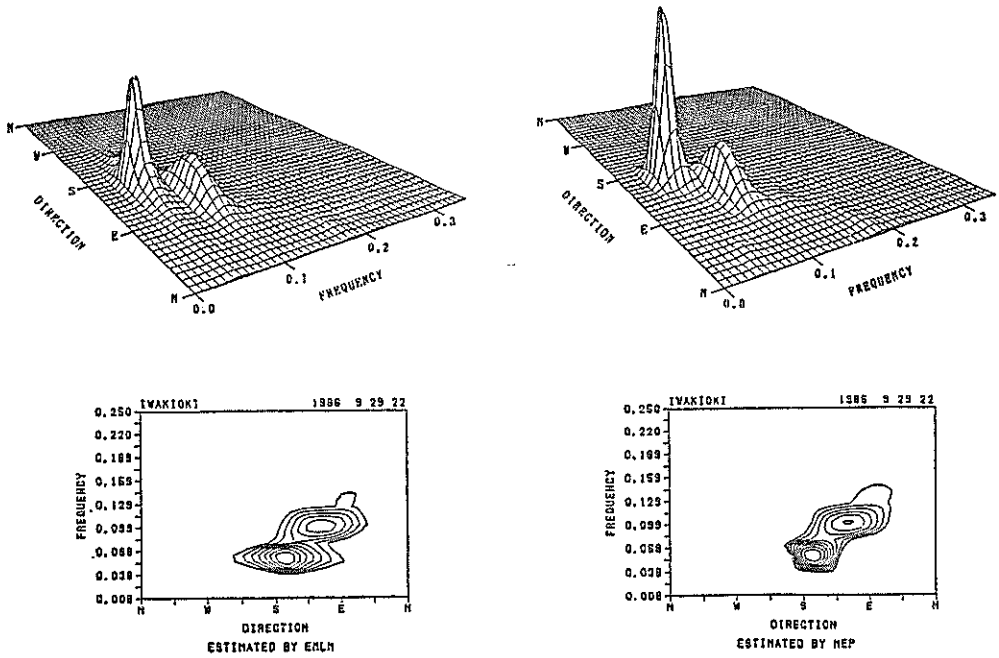

Fig. 22 Bi-directional spectrum observed at 22: 00, 29 Sept. 1986 (3-element measurement)

element measurement detects the directions in which the spectral peaks appear, in uni-directional and bi-directional seas, many wave properties must be measured for a detailed analysis of the directional spectrum.

6. Conclusions

The following major conclusions sum up the study:

1. The proposed Bayesian Directional Spectral Estimation Method (BDM) can be applied to the directional wave analysis on the basis of an arbitrary number of wave probes. However, the method needs wave records consisting of at least four elements of wave properties. When only three elements are measured, the Extended Maximum Likelihood Method (EMLM) and the Maximum Entropy Principle Method (MEP) are recommended.
2. When four or more wave probes are employed in the observation, the BDM is the preferred analytical approach. The directional resolution exhibited by the BDM in this circumstance is greater than those shown by either the EMLM or the Direct Fourier Transformation Method (DFT).
3. The BDM is fairly sound against the noises contained in the estimates of the cross-power spectra. When the rate of the noise over the true cross-power spectra is less than 0.05^2, the BDM yields reliable estimates of the directional spectrum. As the rate increases, the estimate given by the BDM becomes flatter than true directional spectrum. This BDM tendency emerges as the method tends to rely on the a priori condition (smooth and continuous), whenever the

given information (cross-power spectra) is not reliable enough. If the rate of noise exceeds 0.05^2, the EMLM fails to yield reasonable estimates while the BDM can distinguish these directions where the true directional spectrum shows its peak density.

4. When the BDM is employed for directional wave measurement utilizing four wave gauges in a star array (Type-2 in Fig. 2), it provides a very accurate estimate for the true directional spreading function without showing any side lobes, even though the distance between the wave gauges is twice the wave length. This accuracy is very advantageous for the observing random ocean waves having various component waves with wide ranges of frequency.
5. Estimates of the directional spectrum vary widely depending on the method employed for the directional wave analysis, number of elements of wave properties to be analyzed and the layout of the probes. Though the directions where the directional spectrum shows its peak density can be detected from the directional wave analysis on the basis of three or four element measurement, it is necessary to measure directional waves with many probes to detail the shape of the directional spectrum. For field observation, especially in deep sea, simultaneous measurements of many wave properties are very difficult for technical and financial reasons. However the BDM is a very powerful method for the directional wave analysis in laboratories.
6. In the present paper, as an a priori condition, the simplest condition is introduced to characterize the inherent nature of the directional spectrum. This is necessary, as the BDM relies heavily on the a priori condition when the given information is insufficient, to delineate the directional spectrum. However, when research reveals more detail in the structure of ocean directional waves, the method can be improved by adopting the newly attained knowledge as the a priori condition. Thus, the BDM is more adaptable to reformulation of estimation equations as the study of structures of directional wave spectrum progresses.

(*Received on November 18, 1987*)

Acknowledgement

The field wave data analyzed herein were contributed by the Onahama Port Construction Office, the Second Port Construction Bureau, Ministry of Transport. The authors sincerely wish to express their appreciation to Mr. *M. Takamatsu*, Director General and Mr. *S. Inoue*, the Former Director General of the Onahama Port Construction Office and the officials of the Office and the Second Port Construction Bureau for their continuous efforts in the planning and the implementation of the ocean wave observation. The authors also wish to express heartfelt thanks to Dr. *M. Ishiguro*, Research Staff of the Institute of Statistical Mathematics for his kind introduction of various references related to the Bayesian approach in the field of statistical analysis.

References

1) AKAIKE, H.: Likelihood and Bayes procedure, Bayesian statistics (Bernardo, J. M., De Groot, M. H., Lindley, D. U. and Smith, A. F. M. eds.) University Press, Valencia, 1980, pp. 143–166.

2) HASHIMOTO, N.: Estimation of directional spectrum from a Bayesian Approach, Rept. of P.H.R.I., Vol. 26, No. 2, 1987, pp. 97–125.
3) GODA, Y.: Random seas and design of maritime structure, University of Tokyo Press, 1985, 323p.
4) HONMA, M. and K. HORIKAWA, eds.: Nearshore dynamics and coastal processes, University of Tokyo Press, 1986, 582p.
5) ISOBE, M., K. KONDO and K. HORIKAWA: Extension of MLM for estimating directional wave spectrum, Proc. Sympo. on Description and Modelling of Directional Seas, Paper No. A-6, 1984, 15p.
6) BARBER, N. F.: The directional resolving power of an array of wave detectors, Ocean Wave Spectra, Prentice Hall, Inc., 1961, pp. 137–150.
7) CAPON, J.: High-resolution frequency-wave-number spectrum analysis, Proc. IEEE, Vol. 57, 1969, pp. 1408–1418.
8) JEFFERYS, E. R.: Comparison of three methods for calculation of directional spectra, Proc. 5th Int. Offshore Mechanics and Arctic Engineering (OMAE) Sympo., Tokyo, Japan, Vol. 1, 1986, pp. 45–50.
9) KOBUNE, K. and N. HASHIMOTO: Estimation of directional spectra from the Maximum Entropy Principle, Proc. 5th Int. Offshore Mechanics and Arctic Engineering (OMAE) Sympo., Tokyo, 1986, pp. 80–85.
10) AKAIKE, H.: Confusions of the concept of the entropy, Mathematical Sciences, No. 259, Science Company Ltd., 1985, pp. 53–57 (in Japanese).
11) HAYASHI, T., T. SUZUKI and H. AKAIKE: Special topics of statistics, Textbook of the University of the Air, Japan Broadcast Publishing Company Ltd., 1986, 236p. (in Japanese).
12) PANICKER, N. N. and L. E. BORGMAN: Enhancement of directional wave spectrum estimate, Proc. 14th Coastal Eng. Conf., Copenhagen, 1974, pp. 258–279.
13) SHIGEMASU, H.: Introduction to Bayesian statistics, University of Tokyo Press, 1985, 225p. (in Japanese).
14) SAKAMOTO, Y.: Categorical data analysis by AIC and ABIC, Kyoritsu Publishing Co. Ltd., 1985, 221p. (in Japanese).
15) ISHIGURO, M. and Y. SAKAMOTO: A Bayesian approach to binary response curve estimation, Ann. Inst. Statist. Math., Vol. 35, Part B, 1983, pp. 115–137.
16) ISHIGURO, M. and E. ARAHATA: A Bayesian spline regression, The Proc. of the Instit. of Statist. Math., Vol. 30, No. 1, 1982, pp. 29–36 (in Japanese).
17) ISHIGURO, M.: How do we analyze complicated phenomena? —on large parametric model—, Proc. of Statist. Math., Vol. 33, No. 2, 1985, pp. 251–256 (in Japanese).
18) ISHIGURO, M.: On the use of multiparameter models in statistical measurement technique, Doctrial Dissertation, Tokyo Univ., 1985.
19) SAKAMOTO, Y., M. ISHIGURO and G. KITAGAWA: Akaike information criterion statistics, D. Reidel Publishing Co., Dordrecht, Holland, 1986.
20) MITSUYASU, H., et al.: Observation of the directional spectrum of ocean waves using a cloverleaf buoy, Jour. Physical Oceanography, Vol. 5, 1975, pp. 750–760.
21) GODA, Y. and Y. SUZUKI: Computation of refraction and diffraction of sea waves with Mitsuyasu's directional spectrum, Tech. Note of P.H.R.I., No. 230, 1977, 45p. (in Japanese).

List of Symbols

AIC : *Akaike's* Information Criterion
ABIC : *Akaike's* Bayesian Information Criterion
$B(p, q)$: *Boltzmann's* entropy
d : Water depth

D	:	The minimum separation distance between a pair of wave gauges
$\boldsymbol{D}$	:	A certain operation matrix
$\boldsymbol{D}(k, \sigma)$	:	Vector composed of transfer function
$\boldsymbol{E}(\boldsymbol{x})$	:	Matrix composed of unknown vector x
f	:	Frequency
$\boldsymbol{F}(\boldsymbol{x})$	:	Vector composed of unknown vector x
g	:	Gravitational acceleration
$G(\theta \mid f)$	:	Directional spreading function for specific frequency f
$\hat{G}(\theta \mid f)$	:	Estimate of directional spreading function
$h_m(f)$	:	Transfer function for several quantities related to wave motions
H	:	*Shannon's* entropy
$H_{1/3}$	:	Significant wave height
$H_i(f, \theta)$	:	Transfer function for several quantities related to wave motions
$H_m(k, \sigma)$	:	Transfer function for several quantities related to wave motions
$\boldsymbol{I}$	:	Unit matrix
$I_k(\theta)$	:	A kind of δ function
k	:	Wave number
$\boldsymbol{k}$	:	Wave number vector
K	:	Number of segments of directional spreading function
L	:	Wave length
$L(\cdot)$	:	Likelihood function
$p(\cdot), q(\cdot)$	:	Probability density function
$p(\cdot \mid \cdot)$	:	Conditional probability density function
$p(\cdot, \cdot)$	:	Joint probability density function
r	:	Ratio of the error added to the cross-power spectra
S	:	Concentration parameter of directional spreading function
$S(f)$	:	Frequency spectrum
$S(k, \sigma)$	:	Wave number frequency spectrum
$S(f, \theta)$	:	Directional spectrum
$T_{1/3}$	:	Significant wave period.
u	:	Hyperparameter
$w(k, k')$	:	Window function
ε	:	Error
η	:	Water surface elevation
η_x	:	Water surface slope (x-direction)
η_y	:	Water surface slope (y-direction)
θ	:	Wave propagation direction
σ	:	Angular frequency or standard deviation
σ^2	:	Variance
$\Phi_{mn}(\cdot)$	:	Cross-power spectrum between the m-th and the n-th wave properties